GFZ

Helmholtz-Zentrum
POTSDAM

HELMHOLTZ-ZENTRUM POTSDAM
DEUTSCHES
GEOFORSCHUNGSZENTRUM

Thomas Reinsch, Guido Blöcher, Stefan Kranz

# Data from the Groß Schönebeck Research Platform 2011-06-01 - 2013-12-31 (Report)

Scientific Technical Report STR15/02 - Data

www.gfz-potsdam.de

HELMHOLTZ
GEMEINSCHAFT

Recommended citation:

Reinsch, T., Blöcher, G., Kranz, S. (2015), Data of the Groß Schönebeck Research Platform 2011-06-01 - 2013-12-31 (Report). *Scientific Technical Report 15/02 - Data, GFZ German Research Centre for Geosciences.*
DOI: http://dx.doi.org/10.2312/GFZ.b103-15021

Supplementary datasets:

Reinsch, Thomas; Blöcher Guido; Kranz, Stefan (2015): Data From The Groß Schönebeck Research Platform 2011-06-01 - 2013-12-31 (Datasets). GFZ German Research Center for Geosciences.
DOI: http://dx.doi.org/10.5880/GFZ.b103-15021.1

The report and the datasets are supplements to:

Blöcher, G. et al. (2015), Hydraulic history and current state of the deep geothermal reservoir Groß Schönebeck. Geothermics.
DOI: http://dx.doi.org/10.1016/j.geothermics.2015.07.008

Imprint

Helmholtz Centre Potsdam
GFZ German Research Centre
for Geosciences

Telegrafenberg
D-14473 Potsdam

Published in Potsdam, Germany
August 2015

ISSN 2190-7110

DOI: http://dx.doi.org/10.2312/GFZ.b103-15021
URN: urn:nbn:de:kobv:b103-15021

This work is published in the GFZ series
Scientific Technical Report (STR)
and electronically available at GFZ website
www.gfz-potsdam.de

Thomas Reinsch, Guido Blöcher, Stefan Kranz

# Data from the Groß Schönebeck Research Platform 2011-06-01 - 2013-12-31 (Report)

Scientific Technical Report STR15/02 - Data

# Data From The Groß Schönebeck Research Platform 2011-06-01 - 2013-12-31 (Report)

Thomas Reinsch (Thomas.Reinsch@gfz-potsdam.de)
Guido Blöcher (Guido.Bloecher@gfz-potsdam.de)
Stefan Kranz (Stefan.Kranz@gfz-potsdam.de)

Helmholtz Centre Potsdam
GFZ German Research Centre for Geosciences

Wednesday 2nd September, 2015

Scientific Technical Report STR 15/02 - Data
DOI: http://dx.doi.org/10.2312/GFZ.b103-15021

Deutsches GeoForschungsZentrum GFZ

# Abstract

This report as well as the associated data is a supplement to the publication Blöcher et al. (2015) accessible via http://dx.doi.org/10.1016/j.geothermics.2015.07.008.

From 2011-06-01 until 2013-12-31, the measurement and control system at the Groß Schönebeck research platform acquired data from several circulation experiments. Different data values were recorded at a sampling interval of 1 s. Relevant data for understanding and analyzing the hydraulic situation of the system were resampled to a 1 minute interval. From the resampled dataset, additional parameters were derived. Furthermore, if parameters were considered to be essential, but the measurement of these parameters was erroneous, some data were reprocessed. All relevant data and processing steps performed on the data are described within this report. Data described within this report can be accessed via DOI:http://dx.doi.org/10.5880/GFZ.b103-15021.1.

The presented data was acquired during different research projects by the staff of the International Centre for Geothermal Research as well as Section 4.1 Reservoirtechnologies at the Helmholtz Centre Potsdam GFZ German Research Centre for Geosciences.

# Contents





Scientific Technical Report STR 15/02 - Data
DOI: http://dx.doi.org/10.2312/GFZ.b103-15021

Scientific Technical Report STR 15/02 - Data
DOI: http://dx.doi.org/10.2312/GFZ.b103-15021

# List of Figures





Scientific Technical Report STR 15/02 - Data
DOI: http://dx.doi.org/10.2312/GFZ.b103-15021
Deutsches GeoForschungsZentrum GFZ

# List of Tables





Scientific Technical Report STR 15/02 - Data
DOI: http://dx.doi.org/10.2312/GFZ.b103-15021
Deutsches GeoForschungsZentrum GFZ

# Part I.

# Geothermal Research Platform



Scientific Technical Report STR 15/02 - Data
DOI: http://dx.doi.org/10.2312/GFZ.b103-15021

# 1. Infrastructure

In Groß Schönebeck, a geothermal well doublet system has been established to investigate the provision of geothermal energy from a deep sedimentary basin in Germany. Here, a well 4400.4 m deep (measured depth (MD)), the GtGrSk 4/05(A2), was used as production well and a former hydrocarbon exploration well, EGrSk 3/90, was used as injection well (4309 m deep, MD). Tables 8.4 and 8.2 list details of the completion of both wells. Tables 8.3 and 8.1 list the position of both wells. Dip and azimuth data are attached as data files. Both wells have been stimulated within the reservoir interval. A detailed description can be found in Legarth et al. (2003, 2005); Zimmermann et al. (2009); Zimmermann and Reinicke (2010); Zimmermann et al. (2010, 2011). During the circulation experiments, the production well GtGrSk 4/05 (A2) was equipped with a Y-tool to allow for logging while production. The set-up of the production string can be seen in Figure 1.1. In order to monitor and control processes relevant for the operation of the geothermal doublet system, a measurement and control system was established at the Groß Schönebeck research site. From all gathered data, a subset was resampled and reprocessed to analyze the hydraulic situation within well and reservoir.

A list of publications related to the Groß Schönebeck site is added to the Appendix.



Scientific Technical Report STR 15/02 - Data
DOI: http://dx.doi.org/10.2312/GFZ.b103-15021
Deutsches GeoForschungsZentrum GFZ

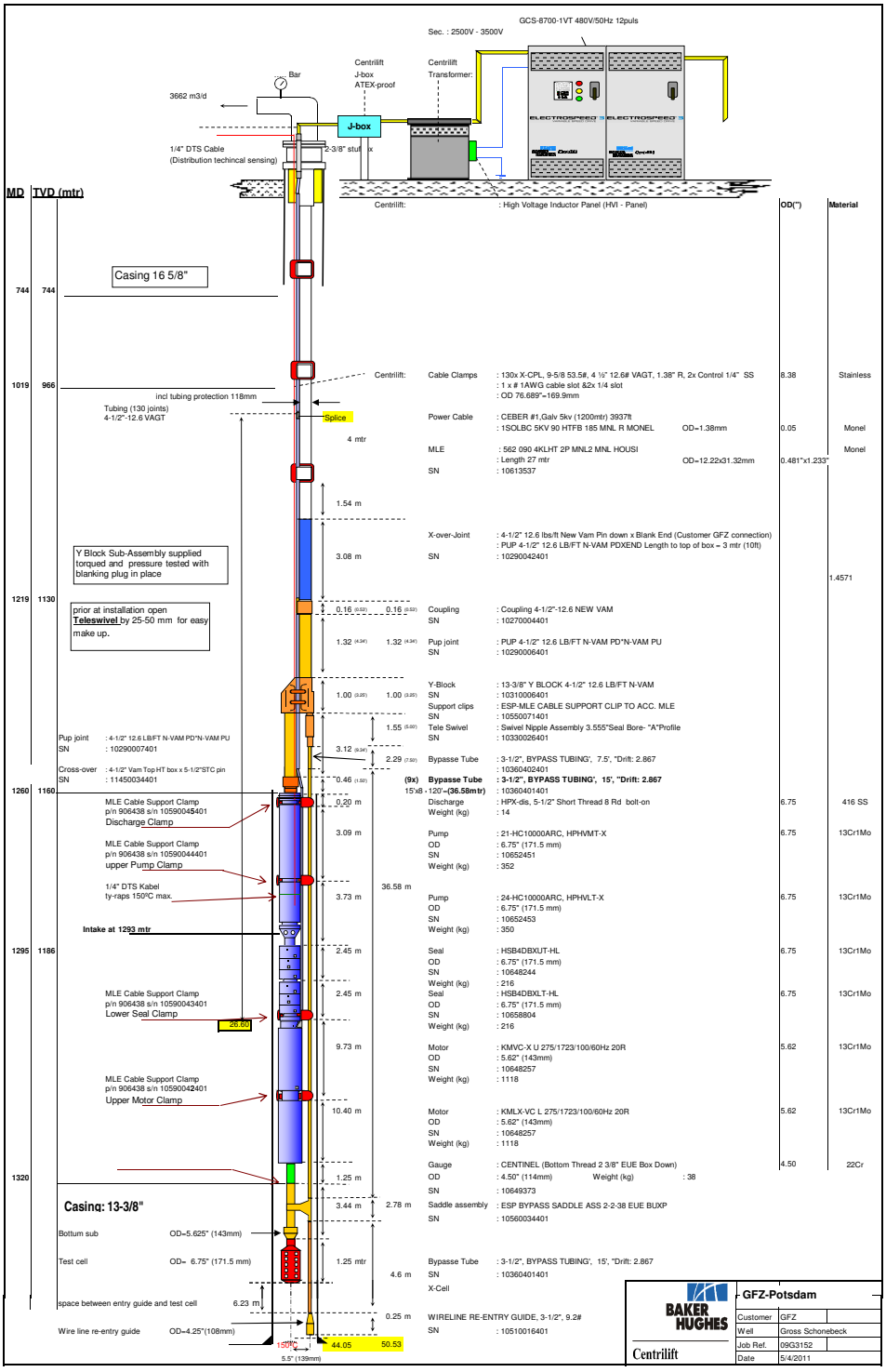


**Figure 1.1.:** Set-up of the production string within the well GtGrSk 4/05 (A2)

# 2. Data Acquisition

The general set-up of the research platform is explained in Frick et al. (2011). From 2011-06-01 to 2013-12-31, several circulation experiments have been performed. A detailed description of the different experiments can be found in Blöcher et al. (2015) (DOI: http://dx.doi.org/10.1016/j.geothermics.2015.07.008). To control and analyse the hydraulic situation within the thermal water loop, several parameters were measured in the system. Figure 2.1 shows the position of different sensors that were used to acquire data during the experiments. Within the Groß Schönebeck plant, liquid flow rates were measured using magneto-inductive flowmeters. Gas flow rates were measured using vortex flowmeters. All data were sampled at 1-2 Hz. The pressure is given in $bar_g$ relative to atmospheric pressure.

During the communication experiment, different tests have been performed (Blöcher et al., 2015, DOI:http://dx.doi.org/10.1016/j.geothermics.2015.07.008). For some tests, the operational set-up has been adjusted. Table 2.1 lists the different experiments that have been performed.

**Table 2.1.:** List of activities in Groß Schönebeck and associated changes to the operational set-up (P=production well, I=injection well). List partly taken from Henninges et al. (2015).

| Begin | End | Well | Operation |
|---|---|---|---|
| 2011-06-15 | 2011-08-29 | P | The gate valve was partly closed. |
| 2011-09-08 | 2011-09-09 | P | Production logging campaign. |
| 2011-11-01 | 2011-11-01 | | The corrosion test rack within equipment facility was included in thermal water loop. |
| 2011-11-20 | 2013-12-31 | | The corrosion test rack outside the equipment facility was included in thermal water loop. |
| 2012-04-02 | 2012-04-17 | P | A bypass was installed at the wellhead. Produced fluid was partly re-injected into the annulus to increase the flow rate at the production pump. |
| 2012-06-20 | | P | p-T log. |
| 2012-07-26 | | P | Bailer run. |
| 2012-08-07 | | I | Bailer run. |
| 2012-08-07 | 2012-08-07 | | Fluid was produced to slop tank and not re-injected in injection well. |
| 2012-09-11 | 2012-10-23 | I | Additional injection of fresh water. |
| 2012-10-24 | | P | p-T log. |
| 2012-11-26 | 2012-12-06 | P | Coiled tubing workover operation. |
| 2012-12-10 | 2012-12-10 | | Fluid was produced to slop tank and not re-injected. |
| 2012-12-12 | 2012-12-12 | | Fluid was produced to slop tank and not re-injected. |
| 2012-12-15 | 2013-12-31 | | The corrosion test rack within the equipment facility was included in thermal water loop. |
| 2012-12-21 | 2012-12-29 | P | Bailer run, multifinger caliper log. |
| 2013-01-10 | | I | p-T log. |
| 2013-06-04 | | I | p-T log. |
| 2013-08-15 | 2013-08-22 | | Calibration measurements gas flow from annulus and degasser. |
| 2013-11-05 | 2013-11-09 | | Fluid was produced to slop tank and not re-injected in injection well. |



Scientific Technical Report STR 15/02 - Data
DOI: http://dx.doi.org/10.2312/GFZ.b103-15021
Deutsches GeoForschungsZentrum GFZ

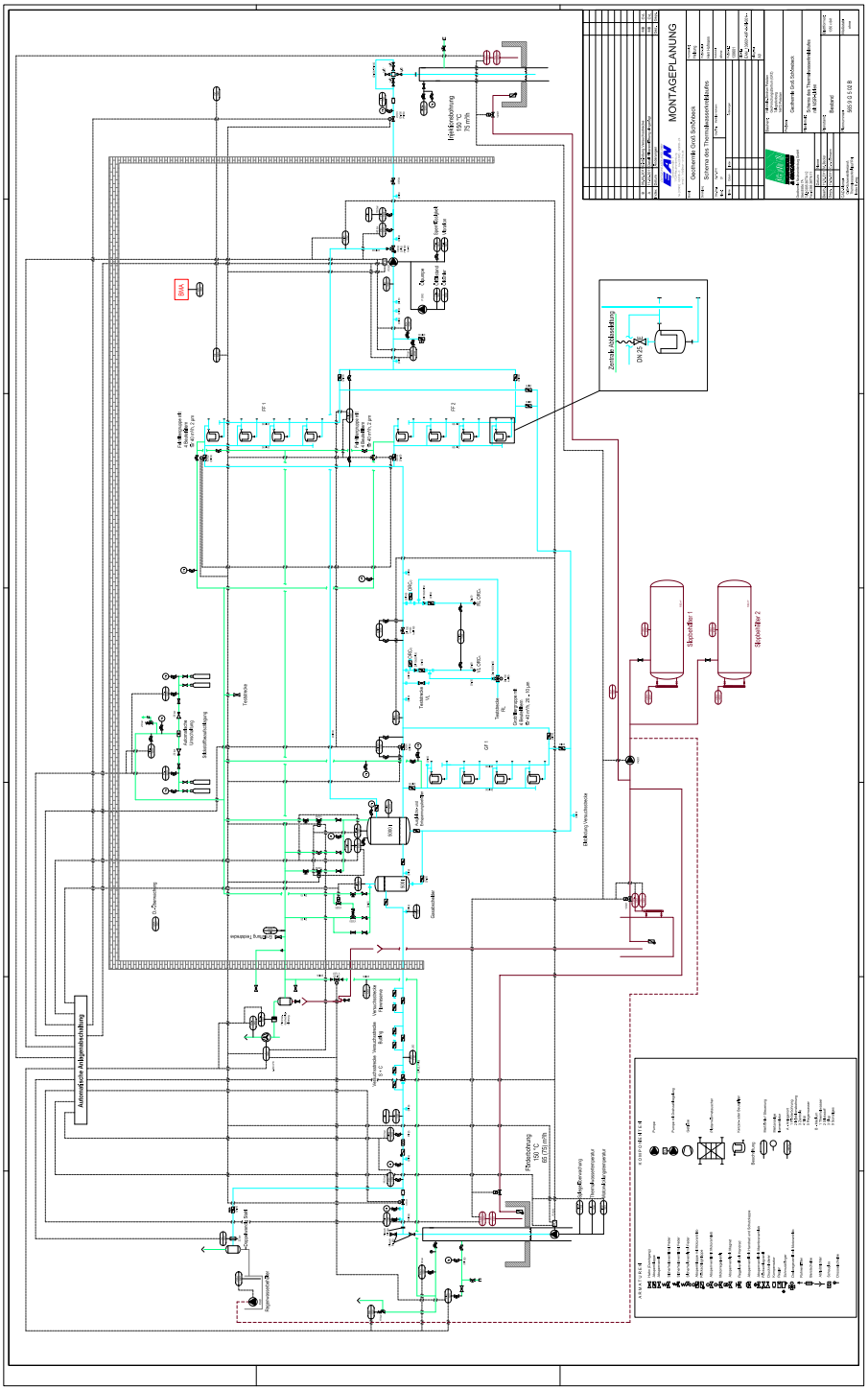


**Figure 2.1.:** Schematic of the thermal water loop and the position of different sensors within the system.



Scientific Technical Report STR 15/02 - Data
DOI: http://dx.doi.org/10.2312/GFZ.b103-15021

# Part II.

# Data



Scientific Technical Report STR 15/02 - Data
DOI: http://dx.doi.org/10.2312/GFZ.b103-15021

# 3. Data Processing

Table 3.1 lists the different sensors and their specific position within the system where data have been resampled for publication. These sensor data are provided as resampled data (type 1) and revised data (type 2). From the resampled data, different quantities were derived. Table 3.1 lists the derived quantities (type 3) that were calculated. All data are provided as comma separated values in separate csv-files. The header of each infividual csv-file corresponds to the sensor name given in Table 3.1. The time range of the data is from 2011-06-01 to 2013-12-31 and all files contain the start time, which is equal for each individual file. Due to the limited number of rows in MS EXCEL the data files were split into two files per quantity. The first file contains data from 2011-06-01 to 2012-07-31 and the second file contains data from 2012-08-01 to 2013-12-31.

Table 3.1.: Description of sensor data and derived quantities. Sensor data are provided as resampled data (type 1) and revised data(type 2). From these sensor data derived quantities (type 3) were calculated.

| Name | Value | Unit | Type | Comment |
|---|---|---|---|---|
| Date_Time | date specification | DD:MM:YYYY hh:mm:ss | 1,2 | |
| PIRS1102 | pressure | bar | 1 | pressure of thermal water in the pipe of production well |
| FIR1201 | flow rate | $m^3/h$ | 1 | gas volume flow rate at production well (annulus) |
| TIR1101 | temperature | °C | 1 | temperature of thermal water on the production side |
| TS3901 | temperature | °C | 1 | temperature at flame arrester behind the degasser |
| FIR3201 | flow rate | $m^3/h$ | 1 | gas volume flow rate in operation hall |
| LIC3101 | liquid level | mm | 1 | level in the degasser (operation hall) |
| LIRC3102 | liquid level | % | 1 | level in surge tank (operation hall) |
| PIR3101 | pressure | bar | 1 | pressure in surge tank (operation hall) |
| TIR3101 | temperature | °C | 1 | temperature of thermal water in surge tank |
| QIR3101 | electrical conductivity | mS/cm | 1 | electrical conductivity of thermal water in the operation hall |
| QRA3102 | amount | % | 1 | oxygen content in air (operation hall) |
| dPIR3102 | pressure difference | bar | 1 | pressure difference across coarse filter |
| dPIRS3103 | pressure difference | bar | 1 | pressure difference across fine filter |
| PIRC3104 | pressure | bar | 1 | pressure of thermal water before injection pump |
| PIR3105 | pressure | bar | 1 | pressure of thermal water after injection pump |
| dPIR3105 | pressure difference | bar | 1 | differential pressure at shut-off valve (operation hall) |
| PS3901 | pressure | bar | 1 | pressure of the sealing liquid at injection pump |
| P3901 | pressure | bar | 1 | air pressure in operation hall |
| T3902 | temperature | °C | 1 | temperature in operation hall |
| TA3301 | temperature | °C | 1 | temperature in slop pit (operation hall) |
| TA1301 | temperature | °C | 1 | temperature in drilling cellar at production well |
| TA2301 | temperature | °C | 1 | temperature in drilling cellar at injection well |
| PIRS1101 | pressure | bar | 1 | wellhead pressure at production well |
| TIR1102 | temperature | °C | 1 | temperature at electric submersible pump |
| TIRS1901 | temperature | °C | 1 | temperature of motor winding at submersible pump |
| Strom_P1101 | electrical current | A | 1 | motor current of electric submersible pump |
| Strom_P3101 | electrical current | A | 1 | motor current of injection pump |
| Strom_L1 | electrical current | A | 2 | current on phase 1 from production pump |

Table 3.1.: Description of sensor data and derived quantities. Sensor data are provided as resampled data (type 1) and revised data(type 2). From these sensor data derived quantities (type 3) were calculated.

| Name | Value | Unit | Type | Comment |
|---|---|---|---|---|
| Strom_L2 | electrical current | A | 2 | current on phase 2 from production pump |
| Strom_L3 | electrical current | A | 2 | current on phase 3 from production pump |
| PIRS1201 | pressure | bar | 2 | annular pressure in production well |
| FIRC3101 | flow rate | $m^3/h$ | 2 | thermal water volume flow rate (operation hall - sum of the volume flow rate from production well and volume flow rate through bypass) |
| PIRS2201 | pressure | bar | 2 | annular pressure in injection well |
| FIR3112 | flow rate | $m^3/h$ | 2 | volume flow rate of thermal water through bypass |
| TIR3102 | temperature | °C | 2 | temperature of thermal water before injection pump |
| PIRS2101 | pressure | bar | 2 | wellhead pressure at injection well |
| PIRS1103 | pressure | bar | 2 | pressure at inlet of electric submersible pump |
| IFWC | volume | $m^3$ | 2 | cumulative volume produced from fresh water wells |
| IFW | flow rate | $m^3/h$ | 3 | flow rate from fresh water wells |
| FIH | flow rate | $m^3/h$ | 3 | liquid volume flow rate at injection well head |
| FIHC | volume | $m^3$ | 3 | cumulative injected liquid volume at well head |
| FPH | flow rate | $m^3/h$ | 3 | liquid volume flow rate at production well head |
| FPHC | volume | $m^3$ | 3 | cumulative produced liquid volume at well head |
| FPA | flow rate | $m^3/h$ | 3 | liquid volume flow rate in annulus/tubing at production well |
| FPR | flow rate | $m^3/h$ | 3 | liquid volume flow rate from reservoir |
| FPRC | volume | $m^3$ | 3 | cumulative produced liquid volume from reservoir |
| PIRS_WS | pressure | bar | 3 | pressure due to water column in annulus between production string and casing at inlet of ESP |
| Strom_A | current | A | 3 | average current from production pump |
| PIRS2101_C | pressure | bar | 3 | corrected wellhead pressure at injection well |
| FPGD | flow rate | $m^3/h$ | 3 | gas volume flow rate from the degasser at standard conditions (1.013 bar, 293 K) |
| FPGA | flow rate | $m^3/h$ | 3 | gas volume flow rate from the annulus of the production well at standard conditions (1.013 bar, 293 K) |

## 3.1. Resampled data (type 1)

Although the original sampling rate was 0.5 to 1 sec, average values of 1 minute are provided. All resampled data include data gaps and default values of the various sensors due to shut-off times or maintenance service, as these data gaps and default values were not corrected.

## 3.2. Revised data (type 2)

Some data of type 1 were manually revised. The revised data are similar to data of type 1 except that all data gaps were filled by linear interpolation. Data are provided with a temporal resolution of 1 min. The individual data processing steps are given for each file:

- Data gaps for electrical current 1, 2 and 3 (`Strom_L1`, `Strom_L2` and `Strom_L3`) were linearly interpolated.
- Data gaps of annular pressure in the production well (`PIRS1201`) were linearly interpolated.
- Data gaps of the fluid volume flow rate in the operation hall (`FIRC3101`) were linearly interpolated. The liquid volume flow rate measured in the operation hall corresponds to the sum of the liquid flow from the production well and of the liquid flow through the bypass. All values below 0 and above 99 were replaced by 0.
- Data gaps of the annulus pressure in the injection well (`PIRS2201`) were linearly interpolated.
- Data gaps of the volume flow rate of thermal water through bypass (`FIR3112`) were linearly interpolated. All values below 0 and above 99 were replaced by 0.
- Data gaps of the temperature of thermal water before injection pump were linearly interpolated (`TIR3102`). All temperature values below 0 °C were replaced by 0 °C.
- Data gaps of the wellhead pressure at injection well (`PIRS2101`) were linearly interpolated.
- Data gaps of the pressure at electric submersible pump (`PIRS1103`) were linearly interpolated. All pressure values below 0 were replaced by linear interpolation. After turning off the submersible pump, occasionally pressure values were not recorded and default values were stored instead. These default values were replaced by linear interpolation.



Scientific Technical Report STR 15/02 - Data
DOI: http://dx.doi.org/10.2312/GFZ.b103-15021

- For the injection experiments in September/October 2012, additional liquid has been injected from a nearby fresh water well. For the fresh water well the cumulative volume (IFWC) has been measured and data gaps were linearly interpolated. Occasionally, the measured cumulative volume at a given time t drops. This indicates erroneous data. In this case all volumes before with higher cumulative volumes were replaced by the measured volume at t.

## 3.3. Derived quantities (type 3)

From data of type 1 and 2, further quantities were derived. The calculation of each quantity is given below:

- The flow rate from fresh water wells (IFW) in September/October 2012 has been calculated as the time derivative of IFWC. In case that the time derivative was larger than 50 $m^3$/h it was replaced by the last value below 50 $m^3$/h as this was the maximum flow rate from the pump.

- The liquid volume flow rate at injection well head (FIH) was calculated as the difference between the fluid volume flow rate in the operation hall (FIRC3101) and the volume flow rate of thermal water through the bypass (FIR3112): FIH = FIRC3101 - FIR3112. All values below 0 were replaced by 0 as only a flow in one direction was possible.

- The cumulative injected liquid volume at well head (FIHC) was calculated as the integral value of the liquid volume flow rate at injection well head (FIH).

- The liquid volume flow rate at production well head (FPH) was calculated as the difference between the fluid volume flow rate in the operation hall (FIRC3101), the volume flow rate of thermal water through bypass (FIR3112) and the volume flow rate from fresh water wells (IFW): FPH = FIRC3101 - FIR3112 - IFW. All values below 0 were replaced by 0.

- The cumulative produced liquid volume at well head (FPHC) was calculated as the integral value of the liquid volume flow rate at production well head (FPH).

- The liquid volume flow rate in annulus/tubing (FPA) at the production well is defined to be positive during production and negative during shut-in periods. The calculation is based on the measured pressure change over time at a depth of 1202 m in the production well (PIRS_WS). If the pressure of the water column in this depth is above 55 bar, then the water table is within the well section with a larger diameter of the casing (16“). The inner diameter of the casing in this section is 0.377 m which corresponds to a cross sectional area of 0.112 $m^2$ $\widehat{=}$ 112 l/m. If the pressure drops below 55 bar then the water table is in the well section having a inner diameter of 0.314 m corresponding to a cross



Scientific Technical Report STR 15/02 - Data
DOI: http://dx.doi.org/10.2312/GFZ.b103-15021
Deutsches GeoForschungsZentrum GFZ

sectional area of 0.077 $m^2$ ≙ 77 l/m (13 3/8“). The production tubing (4 1/2“) has an outer diameter of 0.114 m which corresponds to a cross sectional area of 0.010 $m^2$ ≙ 10 l/m. The inner radius of the production tubing is 0.102 m which corresponds to a cross sectional area of 0.008 $m^2$ ≙ 8 l/m. Furthermore, the volume of the ESP power supply cable is considered, which is installed in the annulus (between casing and production tubing). This cable has a diameter of 0.051 m corresponding to a cross-sectional area of 0.002 $m^2$ ≙ 2 l/m.

In order to calculate the volume flow rate `FPA` the change of water table [m/s] has to be known. This quantity is derived from the changes of pressure of the water column (`PIRS_WS`) at a depth of 1202 m depth. To calculate the water table change, the gravitational acceleration (9.81 $m/s^2$) and a mean density of the thermal water (1170 $kg/m^3$) are used. The density of the thermal water was derived as the average density of the column from the pressure information at the inlet of the ESP. From the slope of the pressure drop during production, the changing internal diameter of the production casing at a depth of about 742 m could be localized. Having the length of the water column as well as the information about the completion, the fluid density could be calculated.

During production, if the pressure at 1202 m is above 55 bar, the liquid level in the annulus drops whereas the production tubing is filled completely. Therefore, the `FPA` can be calculated as the liquid level change over time, taking into account the cross-sectional area of the liquid column. The flow rate can therefore be calculated according to the difference of the inner casing, the power cable and the production tubing 112 l/m - 2 l/m - 10 l/m = 100 l/m. In case of production and a pressure below 55 bar, the flow rate can be calculated according to 77 l/m - 2 l/m - 10 l/m = 65 l/m, taking into account the smaller casing diameter. In the case of a shut-in and a pressure above 55 bar the water table in the annulus and the production tubing raises. Therefore, the `FPA` can be calculated according to 100 l/m + 8 l/m = 108 l/m. In case of shut-in and a pressure below 55 bar the water table raises within the casing of smaller diameter. Therefore, the flow rate can be calculated according to 65 l/m + 8 l/m = 73 l/m.

Immediately shutting down the pump, default values were recorded occasionally. These default values and all values above 100 $m^3/h$ were replaced by linear interpolation.

- The liquid volume flow rate from reservoir (`FPR`) corresponds to the difference between liquid volume flow rate at production well head and liquid volume flow rate in annulus/tubing at production well (`FPH-FPA`).

- The cumulative produced liquid volume from reservoir (`FPRC`) corresponds to the integral over time of the liquid volume flow rate from the reservoir (`FPR`).



Scientific Technical Report STR 15/02 - Data
DOI: http://dx.doi.org/10.2312/GFZ.b103-15021
Deutsches GeoForschungsZentrum GFZ

- The pressure of the water column in the production well (`PIRS_WS`) can be calculated as the difference between the pressure at the inlet of the electric submersible pump and the annular pressure in the production well measured at the wellhead (`PIRS1103 - PIRS1201`)
- The electrical current used to power the electric submersible pump (`Strom_A`) was recorded on all three phases. These values were averaged and used to determine if the ESP was turned on (>=100 A) or off(<100 A).
- In order to correct the wellhead pressure at the injection well (`PIRS2101_C`) a more elaborate calculation had to be performed, which is described in detail in Chapter 4.
- For the calculation of the gas volume flow rate from the degasser (`FPGD`) a more elaborate calculation had to be performed, which is described in detail in Chapter 5.
- For the calculation of the gas volume flow rate from the annulus of the production well (`FPGA`) a more elaborate calculation had to be performed, which is described in detail in Chapter 6.



Scientific Technical Report STR 15/02 - Data
DOI: http://dx.doi.org/10.2312/GFZ.b103-15021
Deutsches GeoForschungsZentrum GFZ

# 4. Corrected wellhead pressure injection well PIRS2101_C

For several circulation experiments, the gate valve at the wellhead of the injection well was partly closed. The wellhead pressure reading PIRS2101, therefore, did not match the actual injection pressure for all experiments as it was installed upstream of the valve. The true wellhead pressure at the injection well can, however, be calculated from other measured quantities.

## 4.1. Theory

Two pressures were recorded at the injection well, namely the wellhead pressure $p_{\mathrm{IB}}$ (PIRS2101) upstream of the gate valve and the annular pressure $p_{\mathrm{IB}}^{\mathrm{RR}}$ (PIRS2201) between casing and injection string at the wellhead. Both values are recorded in $\mathrm{bar_g}$, i.e., relative to the atmospheric pressure. The annulus between casing and injection string is pressurized with gas. The liquid level in the injection string during shut-in periods is therefore higher than in the annulus, whereas the pressure difference corresponds to the liquid level difference. During injection, the liquid level within the injection string, initially at about 230 m below surface, rose to the surface. The annular gas is therefore compressed due to the increasing fluid pressure in the injection string. The length of the gas filled annulus can be calculated from the pressure readings $p_{\mathrm{IB}}$ and $p_{\mathrm{IB}}^{\mathrm{RR}}$, assuming that the fluid and gas density as well is known and the mass of gas is constant. The length can be calculated if $p^{\mathrm{IB}} > 0$, i.e., the liquid level is above the surface and if the gate valve is fully open. To calculate the length of the gas filled annulus, data from the shut-in period following the injection can be used. After shutting down the injection pump, the pressures before and after the gate valve equalize. $p_{\mathrm{IB}}$, therefore can be used to calculate the length of the gas filled annulus. Knowing the amount of gas within the annulus, the injection pressure can be calculated following the procedure given below. Figure 2.1 shows the experimental set-up.

The water table within the annulus (length of the gas filled annulus) $L$ can be calculated for a given density of water $\rho$ according to:

$$L = \frac{(p_{\mathrm{IB}}^{\mathrm{RR}} - p_{\mathrm{IB}})}{\rho g} \tag{4.1}$$

where $g$ is the gravitational acceleration.



Scientific Technical Report STR 15/02 - Data
DOI: http://dx.doi.org/10.2312/GFZ.b103-15021
Deutsches GeoForschungsZentrum GFZ

Knowing the volume and having the information about the annular pressure $p_{\mathrm{IB}}^{\mathrm{RR}}$ (Pa) and temperature within the gas filled annulus $T$ [1], the amount of gas molecules can be calculated according to the ideal gas law. The temperature was assumed to be equal to the fluid temperature measured at the inlet of the injection pump (TIR3102):

$$p_{\mathrm{IB}}^{\mathrm{RR}} V = nRT \tag{4.2}$$

As the area $A$ of the annulus is similar over the entire length of interest, the amount of gas molecules $n^* = \frac{n}{A}$ per area is constant and time independent (given no leakage occurs) and can be calculated together with Equations 4.2 and 4.1 as:

$$n^* = \frac{p_{\mathrm{IB}}^{\mathrm{RR}}(p_{\mathrm{IB}}^{\mathrm{RR}} - p_{\mathrm{IB}})}{\rho g R T} = \text{const.} \tag{4.3}$$

For a given amount of molecules $n^*$ and having information on the wellhead pressure as well as annular pressure together with the annular temperature, the length $L$ of the gas filled annulus can be calculated according to:

$$L = \frac{n^* R T}{p_{\mathrm{IB}}^{\mathrm{RR}}} \tag{4.4}$$

The new wellhead pressure can then be calculated using Equation 4.1 according to:

$$p_{\mathrm{IB}}^{*} = p_{\mathrm{IB}}^{\mathrm{RR}} - L\rho g \tag{4.5}$$

The density of the thermal water has been assumed to be 1170 kg/m$^3$ and the gravity acceleration 9.81 m/s$^2$. To account for the thermal expansion of the water, the density variation is set to be 0.556 kg/(m$^3$ K) at 323 K (from Francke et al., 2013). The isothermal compressibility was neglected.

### 4.1.1. Implementation

In order to estimate the error for the determination of $n^*$, values are calculated for each shut-in period. $n^*$ is calculated for all data points that meet the following three criteria:

- Production pump is off, i.e., a shut-in and zero differential pressure can be assumed across the gate valve
- $p_{\mathrm{IB}} > 0$, i.e., the water table within the injection well is above ground
- $p_{\mathrm{IB}} < p_{\mathrm{IB}}^{\mathrm{RR}}$, i.e., the water table within the annulus is below surface

From the resulting list of data points the average $n^*$ is calculated for each circulation test.

The calculation procedure for each test can therefore be summarized as follows:

[1] Absolute pressure and temperature in Kelvin is needed for calculation.



Scientific Technical Report STR 15/02 - Data
DOI: http://dx.doi.org/10.2312/GFZ.b103-15021
Deutsches GeoForschungsZentrum GFZ

1. Search for data points where: Production pump is off (`Strom_A` $< 100$), $p_{\mathrm{IB}} > 0$ and $p_{\mathrm{IB}} < p_{\mathrm{IB}}^{\mathrm{RR}}$
2. Calculate $n^*$ (Equation 4.3)
3. Calculate statistics on $n^*$
4. Calculate $L$ (Equation 4.4)
5. If the production pump is on, exchange $p_{\mathrm{IB}}$ with $p_{\mathrm{IB}}^*$ (Equation 4.5) for the test preceding the shut-in period.
6. If the production pump is off (`Strom_A` $< 100$) and $p_{\mathrm{IB}} < 0$, $p_{\mathrm{IB}}^*$ can be calculated according to Equation 4.5 throughout the shut-in period.

Figure 4.1 shows the measured $p_{\mathrm{IB}}$ in comparison to the calculated $p_{\mathrm{IB}}^*$ for a communication experiment in April 2012, where the gate valve was partly closed. This is indicated by a higher measured than calculated pressure during the production period. After shutting in, measured and calculated pressures are similar (as the calculated pressure is calibrated to measured pressure). After the water table fell below surface, the calculation procedure still gave reasonable results.

## 4.2. Data Evaluation

The following quantities have been neglected for the calculation:

- Compressibility of fluid (assumed to be small)
- Non-ideal gas conditions
- Weight of the gas column
- Exact position (height) of the pressure sensors
- Exact temperature in different depths
- Loss of annular gas

Although the calculation is simplified, the algorithm gives a reasonable result when compared to results from injection periods with fully opened gate valve. For the beginning of each test, the liquid level in the injection string ( 230 m below surface) rises to the surface. Initially calculated pressure values are therefore negative. For very low annular pressures at the beginning of each test, the algorithm gives values $<$ - 26 $\mathrm{bar_g}$. The comparison of data during production periods, shows that the difference between calculated and measured pressure values (if valve was not partly



Scientific Technical Report STR 15/02 - Data
DOI: http://dx.doi.org/10.2312/GFZ.b103-15021
Deutsches GeoForschungsZentrum GFZ

*4. Corrected wellhead pressure injection well* `PIRS2101_C`

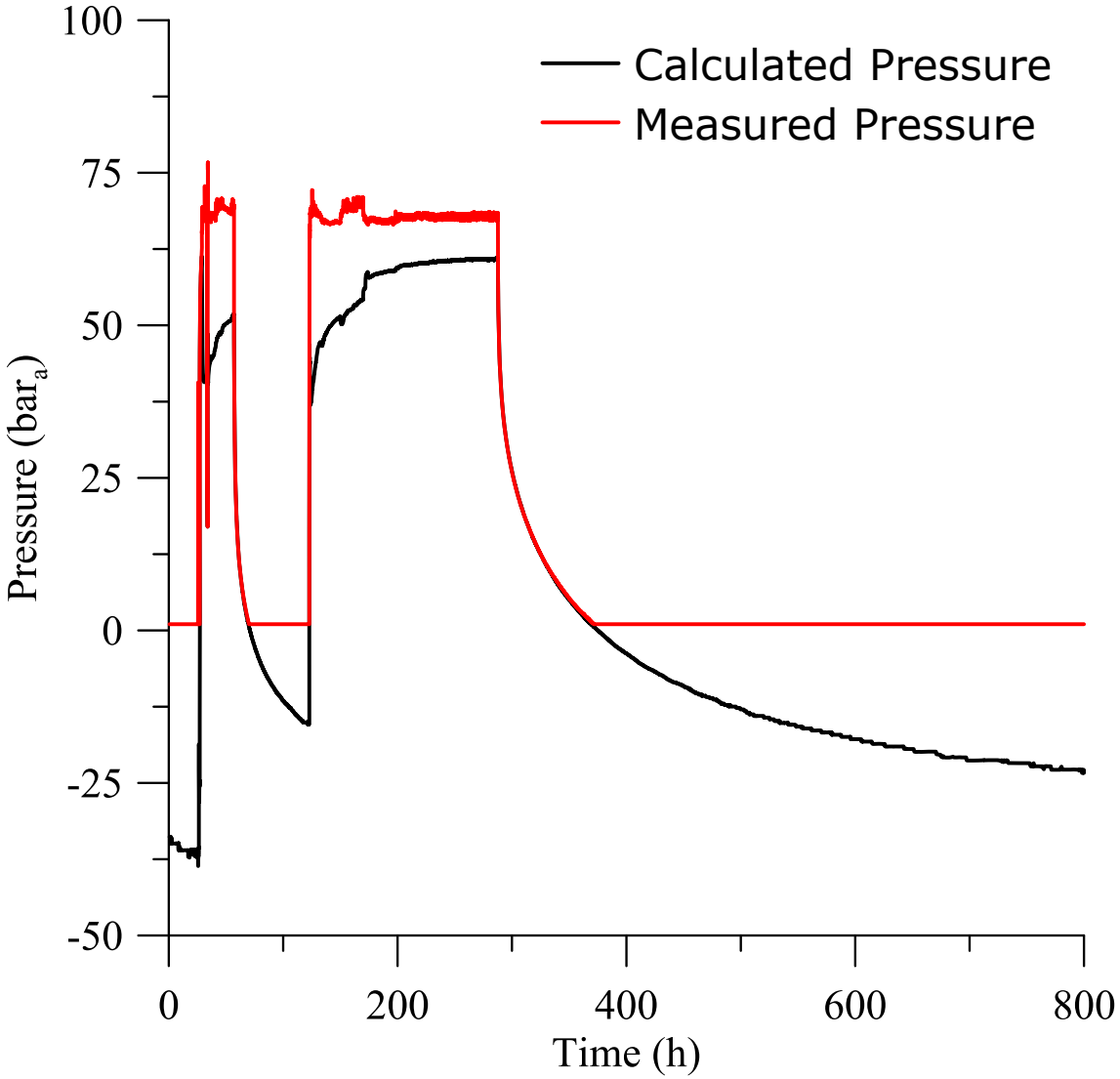


**Figure 4.1.:** Measured $p_{\mathrm{IB}}$ and calculated $p^*_{\mathrm{IB}}$ for a circulation experiment in April 2014.

closed) is below ≈ 1 bar (<2 %) and therefore acceptable. For times with a partly closed valve, a significant difference could be observed.

The procedure outlined above can, in principle, be used to extrapolate the evolution of the liquid level even during very long shut-in times. For very low annular pressures, however, the uncertainty of the calculation is very high. Small changes in the liquid level could hardly be detected using the change of the annular pressure. Here is is advisable to perform at least a single liquid level measurement within the injection string.



Scientific Technical Report STR 15/02 - Data
DOI: http://dx.doi.org/10.2312/GFZ.b103-15021

# 5. Flow rate of gas from the degasser FPGD

The gas flow rate from the degasser was measured by the sensor FIR3201. The FIR3201 is a ProWirl 72F from Endress+Hauser. The sensor is designed to measure the volumetric flow rate of a laminar gas stream for a wide range of flow velocities. The operating principle is a detection of turbulence behind a fin in the gas stream. In Groß Schönebeck the degasser was operated to release gas in short intervals. Within these intervals, the pressure within the gas flow line increased and laminar flow conditions were hardly established. The measured data are therefore erroneous. Furthermore, lacking a pressure and temperature measurement within the gas flow, the mass flow rate could not be calculated. In order to calculate the mass flow rate, the level changes within the degasser between successive releases of gas were used according to the procedure outlined below.

## 5.1. Theory

The calculation of the gas flow rate is based on the ideal gas law (approximately 0.86/0.14 nitrogen/methane mixture, (see e.g. Regenspurg et al., 2010)). To calculate the flow rate, the degasser is assumed to act as a communicating pipe with the surge tank. Pressure and temperature conditions within the degasser are assumed to be equal to the conditions within the surge tank ($T_d = T_s$ (TIR3101), $p_d = p_s$ (PIR3101)).

Within the degasser, the liquid level is recorded continuously (LIRC3102). A level of $h$=600 mm corresponds to a gas volume of $V_d^{gas}$=100.26 l (pers. communication Manfred Hoyer, FAUDI GmbH, 2012-11-01). The inner radius of the degasser is $r$=315 mm. Hence, the volume change within the degasser can be calculated according to:

$$\Delta V = \pi r^2 \Delta h \tag{5.1}$$

Together with the pressure and temperature within the degasser, $p_d(\mathrm{bar_a})$ and $T_d(\mathrm{K})$, the amount of gas can be calculated according to the ideal gas law ($nR = const.$).

$$pV = nRT \tag{5.2}$$

Therefore, the amount of gas within the degasser can be calculated at standard



Scientific Technical Report STR 15/02 - Data
DOI: http://dx.doi.org/10.2312/GFZ.b103-15021
Deutsches GeoForschungsZentrum GFZ

**Figure 5.1.:** Experimental set-up for measuring the gas volume flow rate at atmospheric conditions. The sensor was installed at the end of the flow line, temporarily replacing the flame arrester (Flammdurchschlagsventil).

conditions (1 $\mathrm{bar_a}$, 293.15 K):

$$\frac{p_d V_d^{gas}(T_d, p_d)}{T_d} \frac{293\ \mathrm{K}}{1\ \mathrm{bar}} = V_d^{gas}(293\mathrm{K}, 1\mathrm{bar_a}) \tag{5.3}$$

## 5.2. Validation

### 5.2.1. Set-up

In order to validate the approach, two validation measurements have been performed on the 2013-08-16 and 2013-08-21, respectively. A rotary displacement meter (Drehkolbenzähler) RM-A G250 has been rented (see Appendix). The experimental setup can be seen in Figure 5.1. Furthermore, an additional pressure and temperature sensor has been installed to measure $p$ (within the flow line) and $T$ (on the outside of the flow line) within the gas flow (Figure 5.2). Pictures of the sensors installation can be found in the Appendix. The degasser was repeatedly filled with



Scientific Technical Report STR 15/02 - Data
DOI: http://dx.doi.org/10.2312/GFZ.b103-15021

**Table 5.1.:** Comparison of measured volumes from different degassing cycles for the RM-A G250, FIR3201 (not normalized) and volumes calculated from the fluid level within the degasser on the 2013-08-16.

| | RM-A-G250 ($m^3$) | FIR3201 ($m^3$) | Calculated ($m^3$) |
|---|---|---|---|
| | 1.00 | 0.35 | 0.98 |
| | 1.00 | 0.41 | 1.01 |
| | 0.95 | 0.46 | 0.98 |
| | 0.97 | 0.64 | 1.01 |
| | 0.93 | 0.59 | 1.01 |
| | 1.00 | 0.57 | 1.04 |
| | 1.10 | 0.69 | 1.29 |
| | 1.05 | 0.65 | 1.15 |
| | 1.15 | 0.71 | 1.31 |
| Sum | 9.15 | 5.05 | 9.79 |

nitrogen after releasing the gas for the flow measurement. Data was measured with the different available sensor systems.

### 5.2.2. Results

Table 5.1 compares data from the RM-A G250 and the FIR3201 with calculated values for a measurement at the 2013-08-16. For the measurement, the degasser was manually filled with nitrogen and gas was manually released as well, simulating operational conditions of the thermal water loop. Pressure within the thermal water loop was about 8 - 8.5 $bar_g$. The difference between measured and calculated values is less than 7 % FOR THE RM-A G250. For the sensor FIR3201, it is about 45 %. Normalizing the measured flow rate measured at the FIR3201 according to the measured p-T condition, could not significantly reduce the error, as measured pressure increase during gas release is relatively low.

Table 5.2 compares data from the RM-A G250 and the FIR3201 with calculated values for the measurement at 2013-08-21. Pressure within the thermal water loop was about 5.5 $bar_g$ during the first test and 7.5 $bar_g$ for the second test. The difference between measured and calculated values is less than 10 %. For the sensor FIR3201, it is about 47 %. Normalizing the measured flow rate according to the measured p-T conditions could not significantly reduce the error, as measured pressure increase during gas release is relatively low. Calculating volumes at standard conditions decreased the error to about 41 %.



Scientific Technical Report STR 15/02 - Data
DOI: http://dx.doi.org/10.2312/GFZ.b103-15021
Deutsches GeoForschungsZentrum GFZ

*5. Flow rate of gas from the degasser* `FPGD`

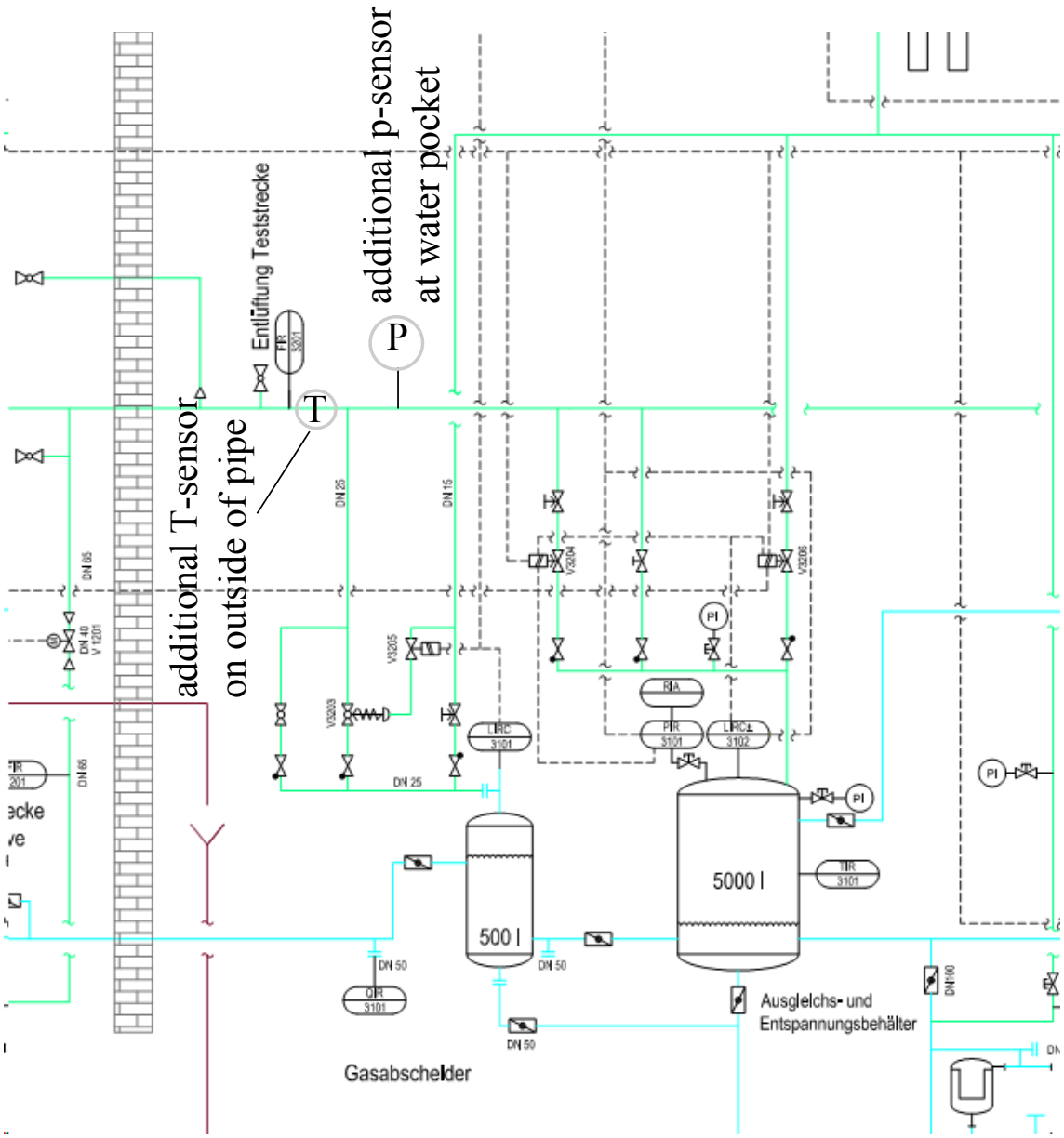


**Figure 5.2.:** Position of additional p-T sensors within the flow line.

**Table 5.2.:** Comparison of measured volumes from different simulated degassing cycles for the RM-A G250 on the 2013-08-21, `FIR3201` (not normalized) and volumes calculated from the fluid level within the degasser.

| | RM-A-G250 ($m^3$) | Calculated ($m^3$) | `FIR3201` ($m^3$) |
|---|---|---|---|
| | 0.78 | 0.831 | 0.27 |
| | 0.75 | 0.787 | 0.31 |
| | 0.90 | 0.916 | 0.45 |
| | 0.90 | 0.931 | 0.49 |
| | 0.87 | 0.925 | 0.47 |
| | 0.80 | 1.011 | 0.56 |
| | 1.03 | 1.086 | 0.59 |
| | 1.00 | 1.112 | 0.55 |
| | 0.98 | 1.09 | 0.54 |
| Sum | 8.01 | 8.69 | 4.23 |
| | 1.02 | 1.069 | 0.31 |
| | 0.98 | 1.024 | 0.38 |
| | 1.00 | 1.065 | 0.44 |
| | 0.94 | 0.995 | 0.58 |
| | 1.02 | 1.128 | 0.66 |
| | 0.88 | 0.972 | 0.5 |
| | 0.95 | 1.085 | 0.56 |
| | 0.83 | 0.981 | 0.52 |
| | 0.88 | 1.06 | 0.56 |
| Sum | 8.50 | 9.38 | 4.51 |
| Sum | 16.51 | 18.07 | 8.74 |



Scientific Technical Report STR 15/02 - Data
DOI: http://dx.doi.org/10.2312/GFZ.b103-15021

### 5.2.3. Discussion

The calculated volume corresponds well to the measured volume at the RM-A-G250. The FIR3201 is eroneous by a factor of 2. Calculating at standard conditions did not significantly reduce the error. It has to be concluded, that the FIR3201 is not suited to measure the flow rate during short gas pulses from the degasser.

## 5.3. Results

The gas fkow rate during the one-week production test in April 2012 is displayed together with the flow rate at the production pump based on data with a resolution of 1 s.

Comparing the results of measured and calculated volumes for the one-week circulation in April 2012, a volume of 1852 $m^3$ has been calculated and a volume of 1030 $m^3$ has been measured at the FIR3201.

### 5.3.1. Error Evaluation

- The assumption of an ideal gas is not valid at elevated pressures. For pressures below 10 bar, however, it is negligible compared to the error of 10% for the calculation.
- Rapid depressurization might lead to different gas temperatures within the degasser than in the surge tank during gas release.
- Gas data are calculated only for times when it accumulated within the degasser, indicated by a falling liquid level. Times of gas release were linearly interpolated between before and after the gas release.

## 5.4. Discussion

Calculated data are consistent with measured data from the RM-A-G250 within an error range of below 10 %. Data from the FIR3201 show a consistent offset (two calibrations and test in April 2014).

For the entire time of production, gas flow data have been averaged to 1 min values. Data from time of gas release have been interpolated.

At certain times, the gas flow rate could not be calculated from the fluid level. This is especially the case for the very beginning of the circulation experiment, where the degasser was sometimes continuously releasing gas. Furthermore, from December 2013 the FIR3201 had a high noise level, although gas was not released. Therefore, this data could not be used for calculation, as calculation is only valid if the FIR3201 gives values close to zero, i.e., when gas is not released.



Scientific Technical Report STR 15/02 - Data
DOI: http://dx.doi.org/10.2312/GFZ.b103-15021

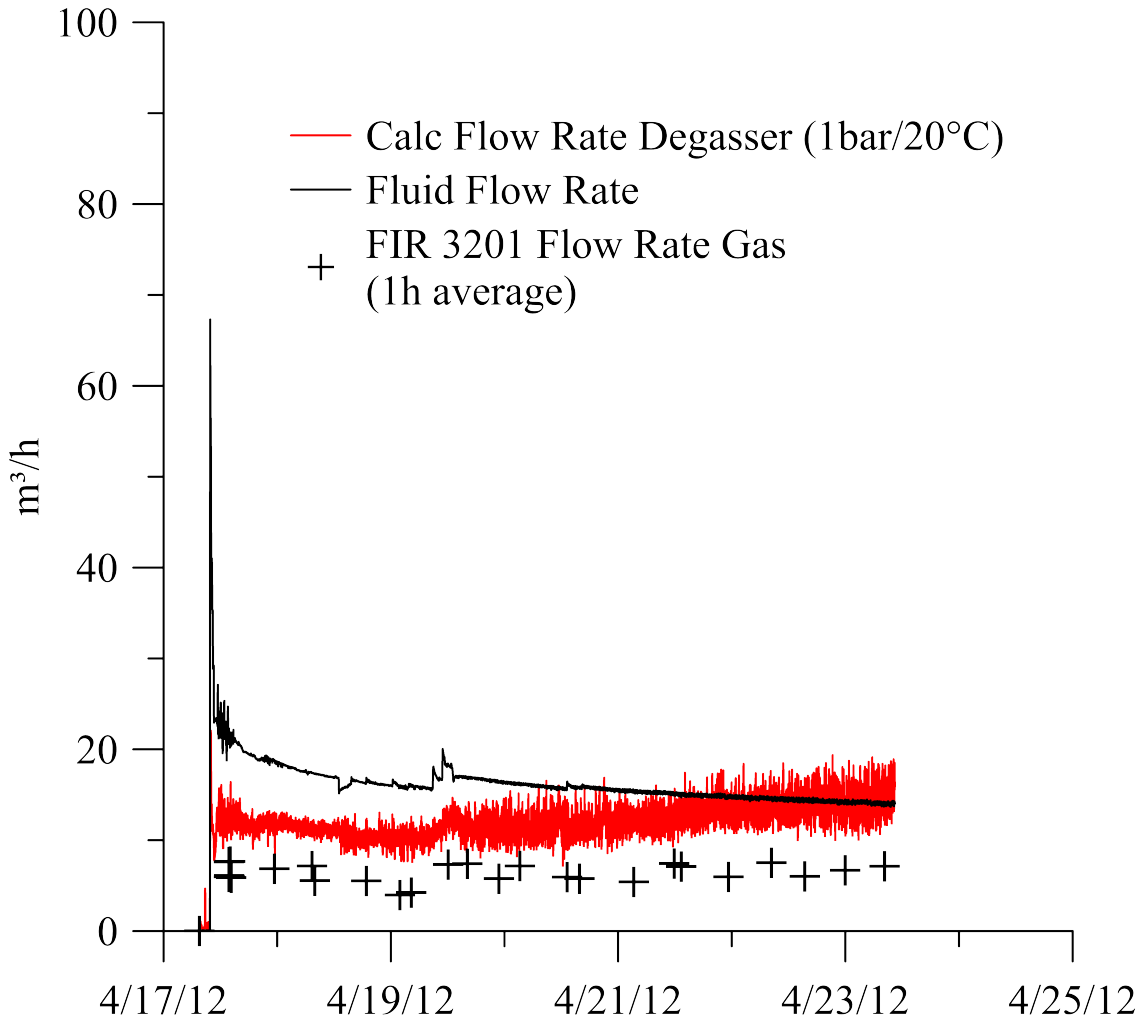


**Figure 5.3.:** Flow rate at production pump together with flow rate of gas at the degasser (normalized to 20 °C, 1 bar). A 25 s moving average is displayed. For comparison, the measured flow rate at `FIR3201` is given as a 1 h average.



Scientific Technical Report STR 15/02 - Data
DOI: http://dx.doi.org/10.2312/GFZ.b103-15021

*5. Flow rate of gas from the degasser* `FPGD`

## 5.5. Output

- `gas-sec-out.dat` Gas flow rate for every second at the degasser.
- `gas-sec-out-avgMin.dat` Averaged gas flow rate for one minute.
- `gas-sec-out-avgMin-short.dat` Averaged gas flow rate over one minute from 2011-09-08 10:31:00.000 to 2012-12-13 16:37:00.000 as this is data without a lot of missing values (see discussion about times without gas release). There are still 730 out of approx. 35000 data points missing. This gives another error of about 2 %.
- `gas-sec-out-avgMin-short-ExpandTime.dat` Averaged gas flow rate for one minute from 2011-09-08 10:31:00.000 to 2012-12-13 16:37:00.000, times in-between are filled with „x“ in order to indicate times with no operation.

Within the time 2011-09-08 10:31:00.000 to 2012-12-13 16:37:00.000, the `FIR3201` gave a volume of 5453 $m^3$, 8570 $m^3$ have been calculated. This is roughly consistent with the data from the calibration (36 % difference).



Scientific Technical Report STR 15/02 - Data
DOI: http://dx.doi.org/10.2312/GFZ.b103-15021

# 6. Flow rate of gas from the annulus of the production well FPGA

## 6.1. Introduction

The gas release from the well annulus is realised through a 1“ pipe that is connected to the gas release system of the whole brine piping system. The annulus gas pipe has a length of approx. 50 m with several fittings and bows. The gas flow rate was meant to be measured with the FIR1201 flow meter. During operation, gas flow or gas velocity is lower than the operation range of the flow sensor. Hence, the flow meter does not deliver the gas flow rate correctly or even does not detect any flow rate at all, if gas velocity is too low. For the evaluation of the gas flow from the annulus only the annulus pressure, temperature and opening (in %) of the gas release control valve are available. Therefore the following relationship needs to be identified.

$$\dot{m}_{\mathrm{gas}} = f(p_{\mathrm{well}}, t_{\mathrm{well}}, \text{Valve } \%) \tag{6.1}$$

In order to identify the relation between gas flow and available parameters, the following model approach was applied:

1. estimating the pressure change in the gas pipe between wellhead and the control valve with regard to pressure changes due to friction and gas expansion
2. estimating the gas flow behaviour of the control valve

To calibrate the model, a series of measurements was performed on site. Additional sensors for pressure, temperature and volume flow rate were installed. The position of installation is shown in the P&I diagram (orange) in Figure 6.1. The temperature and pressure sensor measured at the inlet of the control valve is used to calculate the pressure difference of the gas pipe system during gas release. The temperature is used for identifying the temperature change during gas expansion. The pressure sensor inside the equipment facility delivers the pressure at which the gas volume flow is measured. The value is needed for gas mass flow calculation and, in addition, to distinguish sonic from subsonic gas flow inside the control valve. The gas flow rate was measured with the sensor RM-A G250 as described in Section 5. The approach to calculate the gas flow rate from teh annulus was taken from Wagner (1996, 2001).



Scientific Technical Report STR 15/02 - Data
DOI: http://dx.doi.org/10.2312/GFZ.b103-15021

6. *Flow rate of gas from the annulus of the production well* `FPGA`

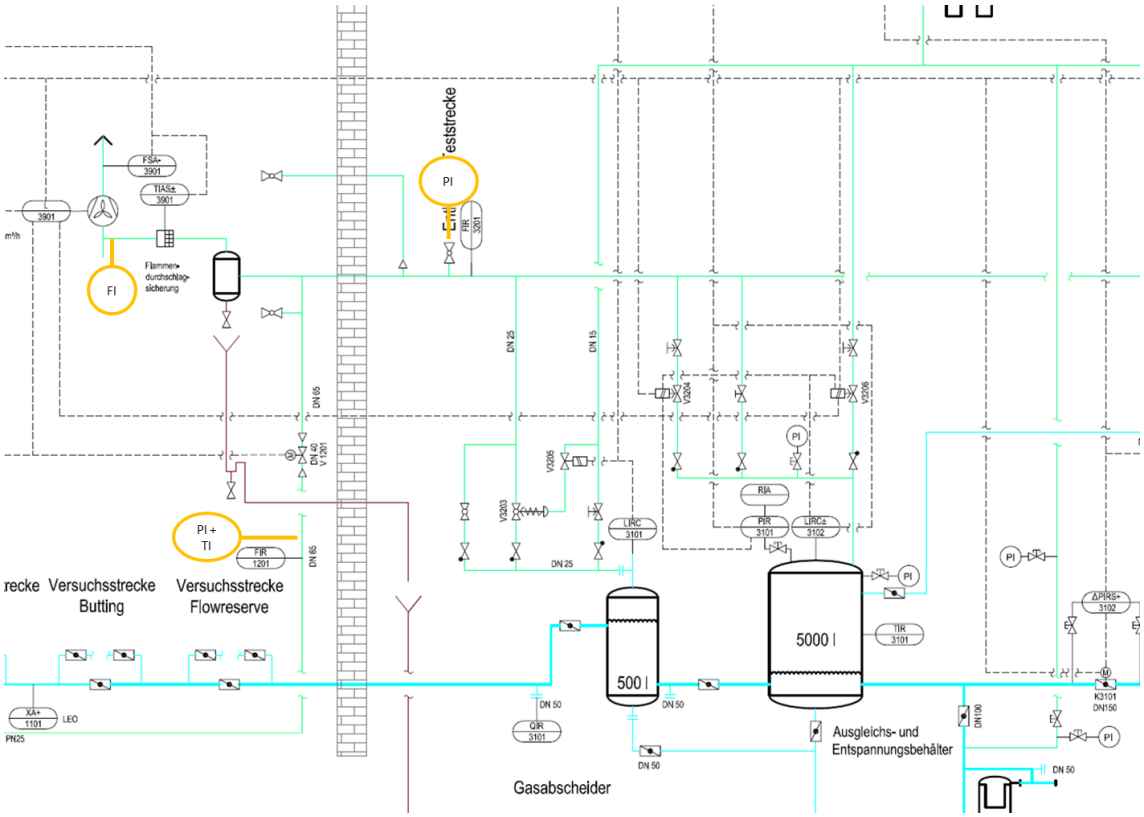


**Figure 6.1.:** PI diagram including the additional sensors.



Scientific Technical Report STR 15/02 - Data
DOI: http://dx.doi.org/10.2312/GFZ.b103-15021

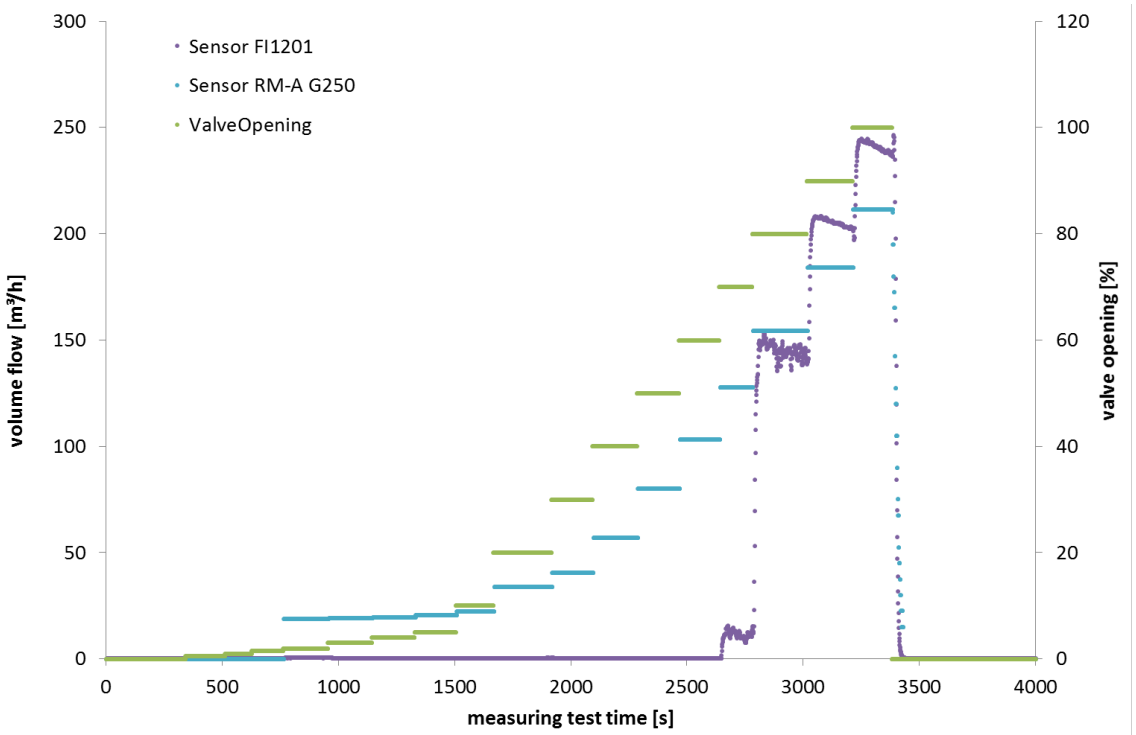


**Figure 6.2.:** Volume flow rate at sensor FIR1201 (purple), sensor RM-A G250 (blue) and valve opening (green).

## 6.2. Validation of installed flow rate sensor FIR1201

In order to determine the accuracy of the installed flow sensor FIR1201, a test with the calibrated flow sensor RM-A G250 was performed. Figure 6.2 shows the comparison of gas flow rate data provided by the FIR1201 and the additionally installed RM-A G250. The volume flow rate at FIR1201 is normalized to 1 bar since the measurement is performed at annular pressure reduced by the pressure change in the gas release pipe. The pressure at RM-A G250 operates almost at ambient conditions. The annular pressure during this test was approximately 11 bar.

During the validation test the valve was opened stepwise beginning at 0 % nd going up to 100 %. The flow rate sensor RM-A G250 could measure a flow rate starting from a valve openings of 2 % and higher. The FIR1201 only detects a flow rate at valve opening greater or equal 50 %, when the flow velocity is within the operating range. The FIR1201 needs a minimum flow velocity of 3 m/s which represents a volume flow rate at the sensor of approx. 20 $m^3/h$.



Scientific Technical Report STR 15/02 - Data
DOI: http://dx.doi.org/10.2312/GFZ.b103-15021

*6. Flow rate of gas from the annulus of the production well* `FPGA`

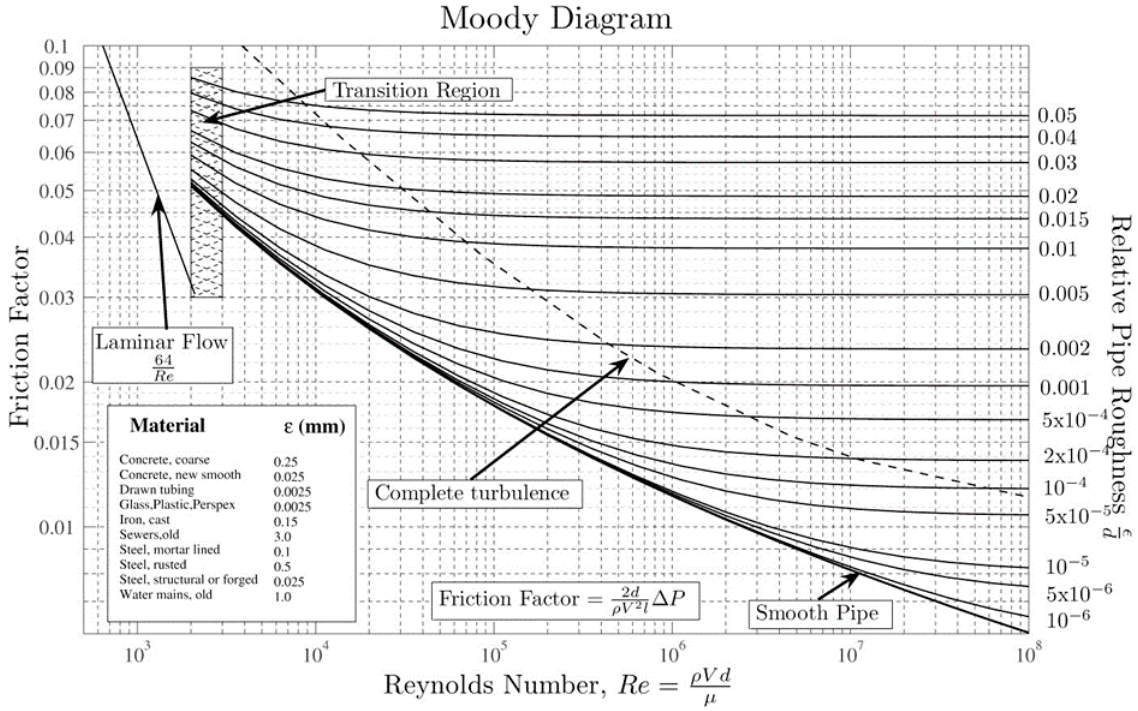


**Figure 6.3.:** Moody diagram (Ingram, 2011).

## 6.3. Pressure change in gas pipe between wellhead and control valve

The approach for calculating the pressure change in the gas release pipe between wellhead and control valve was conceived making the following assumptions:

- The gas state can be calculated applying the ideal gas law.
- Gas flow inside the pipe is always subsonic: Mach number<1.
- Flow is completely turbulent i.e., $\lambda \sim \epsilon/d$. $\lambda$ is called the friction factor and is constant for an existing pipe if $\epsilon$ (surface roughness) and $d$ (pipe diameter) are constant (Moody diagram Figure 6.3 for completely turbulent flow).

The simplified approach by Wagner (2001) is used to calculate the pressure change between pipe inlet and outlet.

$$\Delta p = p_{\text{in}} \left( 1 - \sqrt{1 - \lambda \frac{l}{d} \frac{\rho_{\text{in}}}{2} w_{\text{in}}^2 \frac{2}{p_{\text{in}}} \frac{T}{T_{\text{in}}}} \right) \tag{6.2}$$



Scientific Technical Report STR 15/02 - Data
DOI: http://dx.doi.org/10.2312/GFZ.b103-15021
Deutsches GeoForschungsZentrum GFZ

The term $\lambda \cdot l/d$ represents the pressure drop due to friction and can be considered constant and the flow in the pipe is fully turbulent. The term can be summarized as one parameter $\zeta$.

$$\Delta p = p_{\text{in}} \left( 1 - \sqrt{1 - \zeta \frac{\rho_{\text{in}}}{2} w_{\text{in}}^2 \frac{2}{p_{\text{in}}} \frac{T}{T_{\text{in}}}} \right) \tag{6.3}$$

Solving for $\zeta$ yields to:

$$\zeta = \left( 1 - \left( 1 - \frac{\Delta p}{p} \right)^2 \right) \frac{T_{\text{in}} p_{\text{in}}}{T \rho_{\text{in}} w_{\text{in}}^2} \tag{6.4}$$

$\zeta$ can be derived from measurement data. For fitting $\zeta$ to the measured data, the method of least squares was used. $p_{\text{in}}$ is pressure at inlet (Pa), $\rho_{\text{in}}$ density at inlet (kg/m$^3$), $w_{\text{in}}$ flow velocity at inlet (m/s), $T$ average temperature between in- and outlet (K), $T = (T_{\text{in}} - T_{\text{out}})/2$ average temperature in valve (arithmetic mean between inlet and outlet) and $T_{(\text{in/out})}$ is inlet and outlet gas temperature (K), respectively.

### 6.3.1. Gas release pipe model calibration

In order to determine the gas dynamic behaviour of the gas release pipe and the control valve, two sets of measurements were performed. The first set was performed at an annular pressure of approx. 10 bar and the second set was performed at an annular pressure of approx. 6 bar. Both pressure levels were chosen to cover the annular pressure range of possible operation conditions. In each series the valve opening was varied between 0 and 100 % as follows: 0, 0.5, 1, 2, 3, 4, 5, 10, 20, 30, 40, 50, 60, 70, 80, 90, 100 %.

The parameter $\zeta$ was determined for the gas pipe connecting the wellhead to the control valve (section 1) and for the pipe section after the control valve (section 2), separately. Model calibration based on measured data using the method of least squares yields $\zeta_1 = 257$ for the first section and $\zeta_1 = 3$ for the second section. Figure 6.4 shows the result of the pressure loss calculation (red) in comparison to measured data (blue). This approach reproduces the pressure loss in the gas release pipe with sufficient accuracy but the deviation is higher at higher flow rates, i.e., higher pressure differences. The standard deviation of the pressure difference for both test series is 0.045 bar.

However, the effect of changing temperature can be neglected if the temperature change is low as shown in Figure 6.4. Therefore it is justified to consider the gas flow in the pipe as isothermal.

The presented gas pipe flow model was also applied for the pressure drop calculation in section 2 of the pipe after the control valve. Knowing $\zeta$ is essential if subsonic



Scientific Technical Report STR 15/02 - Data
DOI: http://dx.doi.org/10.2312/GFZ.b103-15021
Deutsches GeoForschungsZentrum GFZ

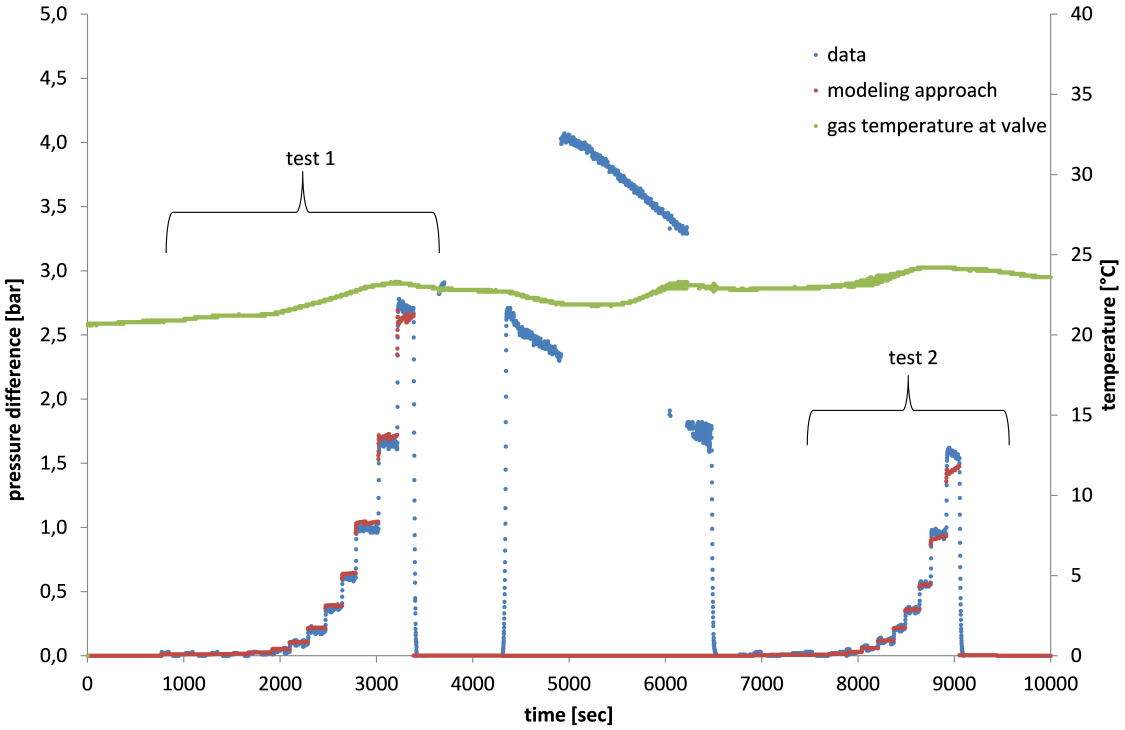


**Figure 6.4.:** Pressure difference in pipe section 1 based on data (blue) and model approach (red).



Scientific Technical Report STR 15/02 - Data
DOI: http://dx.doi.org/10.2312/GFZ.b103-15021

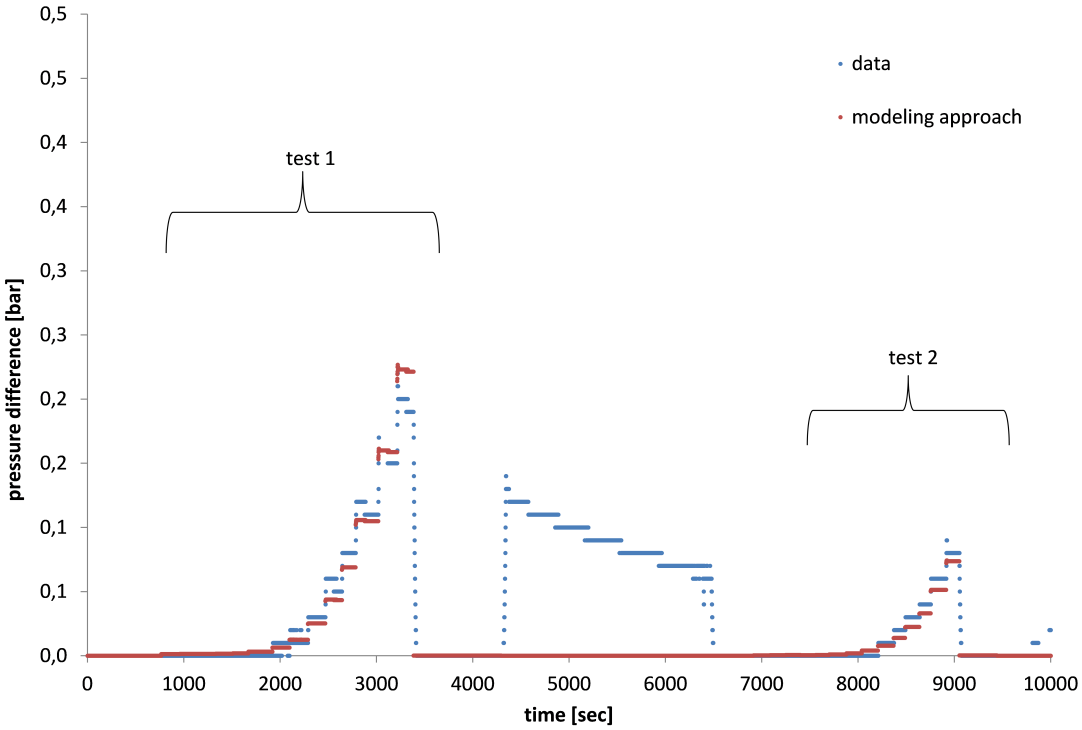


**Figure 6.5.:** Pressure difference in pipe section 2 based on data (blue) and model approach (red).



Scientific Technical Report STR 15/02 - Data
DOI: http://dx.doi.org/10.2312/GFZ.b103-15021

flow in the control valve occurs. In this case the mass flow rate is determined by the pressure difference across the valve. The results of the parameter matching are shown in Figure 6.5. High pressure differences between test 1 and 2 were caused by a high gas flow rate during the annular pressure reduction before the second test.

### 6.3.2. Gas flow across the control valve

Since no sufficient data on the hydraulic or gas dynamic characteristic of the control valve is available, the valve was involved in the testing procedure as well. For developing a modelling approach, the valve was considered to act like a nozzle or orifice representing the smallest cross sectional area in the gas release system. This means that, depending on the pressure difference across the valve, the gas flow might be sonic at the smallest cross sectional area (inside the valve). In that case, the mass flow rate depends on the inlet pressure of the valve only. The flow is sonic as long as the outlet/inlet pressure $p_o/p_i$ ratio complies with the following condition:

$$\frac{p_a}{p_i} < \left(\frac{2}{\kappa+1}\right)^{\frac{\kappa}{\kappa-1}} \tag{6.5}$$

, where $\kappa = c_p/c_v$ is the heat capacity ratio. If $\frac{p_a}{p_i} > \left(\frac{2}{\kappa+1}\right)^{\frac{\kappa}{\kappa-1}}$ the gas flow is subsonic. The mass flow through nozzle is calculated according to:

$$\dot{m} = A\mu\psi\sqrt{2p_i\rho_i} \tag{6.6}$$

Considering the mass flow calculation, the cross sectional area $A$ of the assumed valve and the jet contraction factor $\mu$ are valve specific and they need to be determined. For sonic conditions, the flow parameter $\psi$ can be calculated according to:

$$\psi = \psi_{\max} = \sqrt{\frac{\kappa}{\kappa+1}}\left(\frac{2}{\kappa+1}\right)^{\frac{1}{\kappa-1}} \tag{6.7}$$

$\psi_{\max} = 0.484$ with the heat capacity ratio $\kappa = c_p/c_v = 1.4$ and $p_a/p_i < 0.528$. For subsonic conditions, the flow parameter $\psi$ can be calculated according to:

$$\psi = \sqrt{\frac{\kappa}{\kappa+1}}\sqrt{\left(\frac{p_{\text{out}}}{p_{\text{in}}}\right)^{\frac{2}{\kappa}} - \left(\frac{p_{\text{out}}}{p_{\text{in}}}\right)^{\frac{\kappa+1}{\kappa}}} \tag{6.8}$$

or

$$\psi = \sqrt{\frac{\kappa}{\kappa-1}\left(\frac{p_{\text{out}}}{p_{\text{in}}}\right)^{\frac{1}{\kappa}}\left(\left(\frac{p_{\text{out}}}{p_{\text{in}}}\right)^{\frac{1}{\kappa}} - \frac{p_{\text{out}}}{p_{\text{in}}}\right)} \tag{6.9}$$

$\kappa$ is $\approx 1.4$ $(1.38 - 1.4)$ for an 0.86/0.14 nitrogen/methane mixture according to the NIST REFPROP Database (Lemmon et al., 2007), $\rho = 1.08$ kg/m$^3$ at 293 K and 1 bar.



Scientific Technical Report STR 15/02 - Data
DOI: http://dx.doi.org/10.2312/GFZ.b103-15021
Deutsches GeoForschungsZentrum GFZ

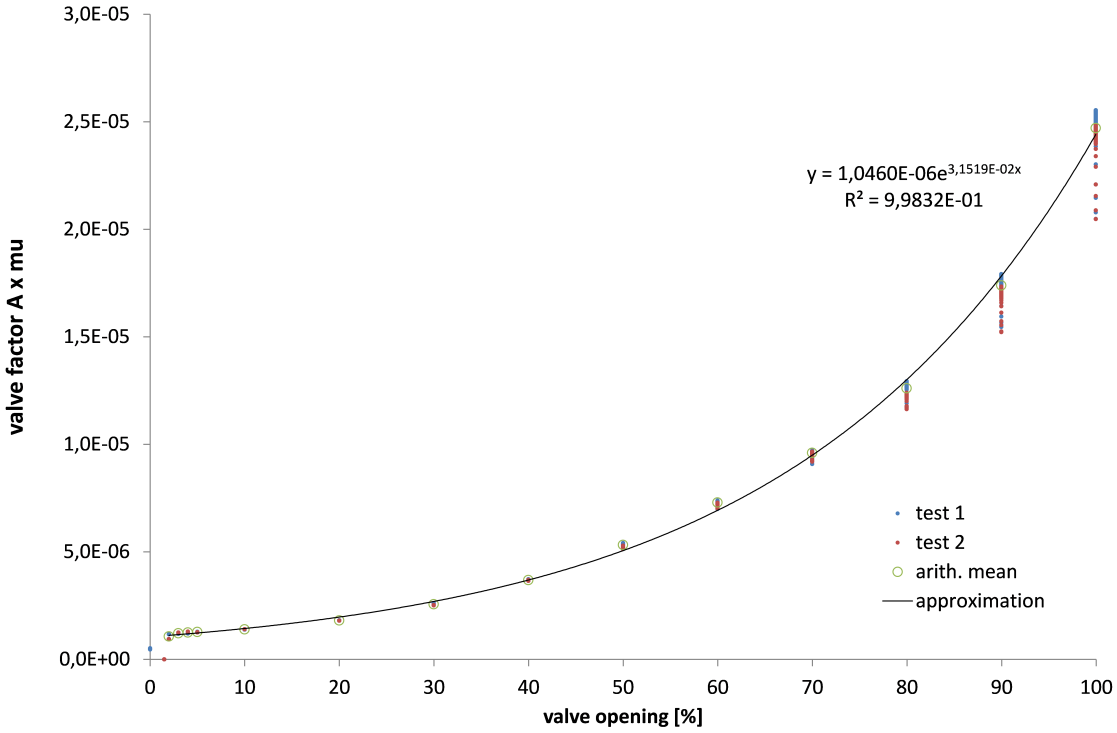


**Figure 6.6.:** Valve parameter as a function of valve opening.

The separate determination of both parameters $A$ and $\mu$ based on measured data is not possible. Therefore both parameters are combined in one "valve parameter". This valve parameter is a function of the valve opening and this function was determined based on measured data.

$$A\mu = f(\text{Valve Opening}) \tag{6.10}$$

$$A\mu = \frac{\dot{m}}{\psi\sqrt{2p_i\rho_i}} \tag{6.11}$$

The "valve parameter" was calculated for each valve opening in both test series. The results are shown in Figure 6.6 and the valve parameter can be approximated by the following exponential function.

$$A\mu = 1.046 \cdot 10^{-6} e^{0.031519y},\ y = \text{Valve Opening in \%} \tag{6.12}$$

During the test series gas flow was detected for a valve opening of less than 2 %, independently from annular pressure. Therefore, for the data analysis, the derived function was only applied within an opening range between 2-100 %. Below 2 %, the gas flow was considered to be zero.



Scientific Technical Report STR 15/02 - Data
DOI: http://dx.doi.org/10.2312/GFZ.b103-15021
Deutsches GeoForschungsZentrum GFZ

*6. Flow rate of gas from the annulus of the production well* `FPGA`

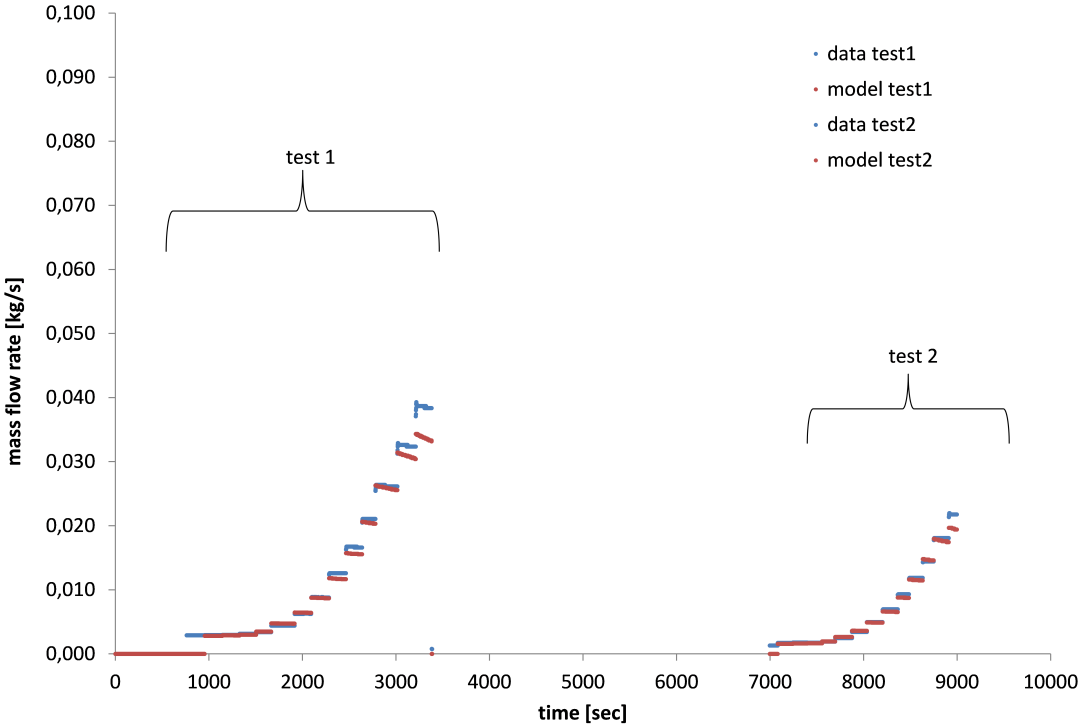


**Figure 6.7.:** Gas mass flow calculation.

## 6.3.3. Gas mass flow calculation

The combination of the gas release pipe model and the control valve model provides an approach to calculate the gas mass flow rate under consideration of the annular pressure, the annular gas temperature and the valve opening. Figure 6.7 shows the results for both test series. The mass flow rate was calculated from the volume flow rate recorded by the flow sensor RM-A G250 and the corresponding gas density for an 0.86/0.14 nitrogen/methane mixture using the following equations.

Mass flow rate (model)

$$\dot{m} = A\mu\psi\sqrt{2p_i\rho_i} \tag{6.13}$$

Mass flow rate (test data):

$$\dot{m} = \dot{V}\rho_2,\ \rho_2 = \frac{p_2\rho_1}{p_1},\ p_1 = 1\ \text{bar},\ \rho_1 = 1.08\ \text{kg/m}^3 \tag{6.14}$$

## 6.3.4. Model implementation and data processing

The derived gas releases flow model was implemented in a Microsoft ACCESS function in Microsoft VBA code in order to process operating data from September to



Scientific Technical Report STR 15/02 - Data
DOI: http://dx.doi.org/10.2312/GFZ.b103-15021
Deutsches GeoForschungsZentrum GFZ

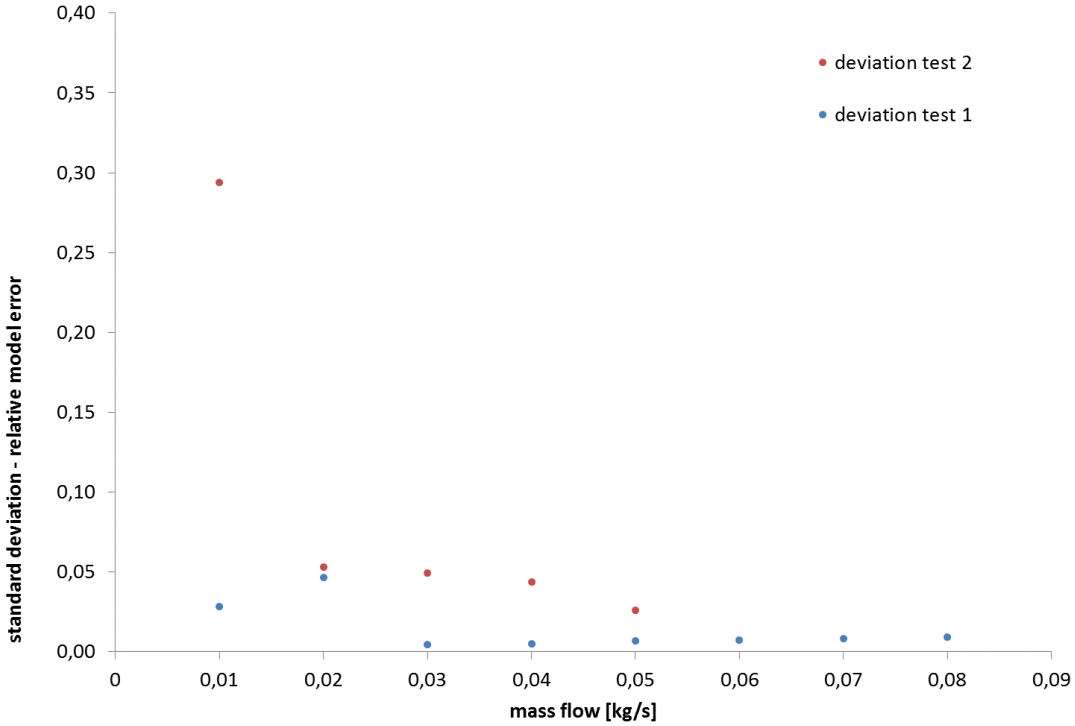


**Figure 6.8.:** Standard deviation of the relative model error.

October 2012. MS ACCESS was used because the raw data were recorded in 1 s intervals and a large data set had to be processed, a task ACCESS is well suited for. The MS VBA function calculates the gas mass flow using annulus pressure, annulus temperature and valve position as inputs.

### 6.3.5. Error estimation

The error which has to be considered when using the derived model for gas mass flow estimation is shown in Figure 6.8. Here the standard deviation of the relative difference between test data and model data is presented. The standard deviation was calculated for different mass flow ranges (0-1; 1-2; 2-3...kg/s). The difference between model and test data is larger for test 2 which was performed at lower annular pressure (6 bar). The lower the mass flow rate the larger is the error. For test 2 the standard deviation of the error is lower than 0.05 in the whole range of mass flow rates between 0 and 0.08 kg/s. Considering gas mass flow calculation based on operating data the large error at low flow rates is less significant since low flow rates do not contribute much to the total gas mass/volume over a given operating time.



Scientific Technical Report STR 15/02 - Data
DOI: http://dx.doi.org/10.2312/GFZ.b103-15021

# Acknowledgement

This work has been performed in the framework of the projects „Nachhaltige Produktion und Injektion von Thermalwasser der tiefen sedimentären geothermischen Lagerstätten Groß Schönebeck“ [BMU, FKZ0325088] and „Qualifizierung geothermischer Technologie - Integration von Untertage- und Übertagesystemen“ [BMU, FKZ0325217], funded by the Federal Ministry for the Environment, Nature Conservation and Nuclear Safety as well as „Langzeit-Korrosionsuntersuchungen und -Monitoring in salinarem Thermalwasser“ [BMWi/BMU, FKZ0325069A] funded by the Federal Ministry of Energy and Economics (BMWi) and the Federal Ministry of Environment, Nature Conversation and Nuclear Safety.

# References


Blöcher, G., T. Reinsch, J. Henninges, H. Francke, H. Milsch, S. Regenspurg, S. Kranz, K. Erbas, C.-T. Rach, A. Saadat, G. Kupfermann, G. Zimmermann, and E. Huenges (2015). Hydraulic history and current state of the deep geothermal reservoir Groß Schönebeck. *Geothermics*. http://dx.doi.org/10.1016/j.geothermics.2015.07.008 (in press).

Brandt, W. (2008). Bohrtechnischer Abschlussbericht für die Bohrung Gt Groß Schönebeck 4 A(2.) (Gt GrSk 4 A(2.)). Technical report, Helmholtz Centre Potsdam GFZ German Research Centre for Geosciences. in German.

Brandt, W. (2009). Technischer Abschlussbericht für die workover – Arbeiten mit coiled tubing 2009 in der Bohrung E Groß Schönebeck 3/90. Technical report, Helmholtz Centre Potsdam GFZ German Research Centre for Geosciences.

Francke, H., A. Saadat, and M. Kumke (2013). Thermal–hydraulic measurements and modelling of the brine circuit in a geothermal well. *Environmental Earth Sciences 70*(8), 3481–3495. http://dx.doi.org/10.1007/s12665-013-2612-8.

Frick, S., S. Regenspurg, S. and Kranz, A. Milsch, H. and Saadat, W. Francke, H. and Brandt, and E. Huenges (2011). Geochemical and process engineering challenges for geothermal power generation. *Chemie Ingenieur Technik 83*, 2093–2104. http://dx.doi.org/10.1002/cite.201100131.

Henninges, J., G. Blöcher, S. Kranz, S. Regenspurg, T. Reinsch, A. Saadat, G. Zimmermannn, and E. Huenges (2015). Reservoir behaviour and borehole processes during egs operation: Experiences from three years of production and injection at the groß schönebeck site. In *Proceedings World Geothermal Congress 2015*, Number 31056.

Ingram, G. (2011). Moody.py. online. http://www.dur.ac.uk/g.l.ingram/download/moody.py (5. May 2011).

Legarth, B., E. Huenges, and G. Zimmermann (2005). Hydraulic fracturing in a sedimentary geothermal reservoir: Results and implications. *International Journal of Rock Mechanics and Mining Sciences 42*(7–8), 1028 – 1041. http://dx.doi.org/10.1016/j.ijrmms.2005.05.014.

Legarth, B., T. Tischner, and E. Huenges (2003). Stimulation experiments in sedimentary, low-enthalpy reservoirs for geothermal power generation, Germany. *Geothermics 32*(4–6), 487 – 495. http://dx.doi.org/10.1016/j.geothermics.2003.07.007.

Lemmon, E. W., M. L. Huber, and M. O. McLinden (2007). *NIST Standard Reference Database 23: Reference Fluid Thermodynamic and Transport Properties-REFPROP, Version 8.0*. Gaithersburg: National Institute of Standards and Technology.

Regenspurg, S., T. Wiersberg, W. Brandt, E. Huenges, A. Saadat, K. Schmidt, and G. Zimmermann (2010). Geochemical properties of saline geothermal fluids from the in-situ geothermal laboratory Groß Schönebeck (germany). *Chemie der Erde - Geochemistry 70, Supplement 3*, 3 – 12. http://dx.doi.org/10.1016/j.chemer.2010.05.002.

Reinsch, T., B. Guido, and S. Kranz (2015). Data from the Groß Schönebeck research platform 2011-06-01 - 2013-12-31 (datasets). Technical report, GFZ German Research Center for Geosciences. http://dx.doi.org/10.5880/GFZ.b103-15021.1.

Wagner, W. (1996). *Regelarmaturen* (1st ed.). Kamprath-Reihe. Würzburg: Vogel Fachbuch.

Wagner, W. (2001). *Strömung und Druckverlust* (5th ed.). Kamprath-Reihe. Würzburg: Vogel Fachbuch.

Zimmermann, G., G. Blöcher, A. Reinicke, and W. Brandt (2011). Rock specific hydraulic fracturing and matrix acidizing to enhance a geothermal system — concepts and field results. *Tectonophysics 503*(1–2), 146 – 154. http://dx.doi.org/10.1016/j.tecto.2010.09.026.

Zimmermann, G., I. Moeck, and G. Blöcher (2010). Cyclic waterfrac stimulation to develop an enhanced geothermal system (egs)—conceptual design and experimental results. *Geothermics 39*(1), 59 – 69. http://dx.doi.org/10.1016/j.geothermics.2009.10.003.

Zimmermann, G. and A. Reinicke (2010). Hydraulic stimulation of a deep sandstone reservoir to develop an enhanced geothermal system: Laboratory and field experiments. *Geothermics 39*(1), 70 – 77. http://dx.doi.org/10.1016/j.geothermics.2009.12.003.

Zimmermann, G., T. Tischner, B. Legarth, and E. Huenges (2009). Pressure-dependent production efficiency of an enhanced geothermal system (egs): Stimulation results and implications for hydraulic fracture treatments. In S. Vinciguerra

and Y. Bernabé (Eds.), *Rock Physics and Natural Hazards*, Pageoph Topical Volumes, pp. 1089–1106. Birkhäuser Basel. http://dx.doi.org/10.1007/978-3-0346-0122-1_16.

# Part III.

# Appendix



Scientific Technical Report STR 15/02 - Data
DOI: http://dx.doi.org/10.2312/GFZ.b103-15021

# 7. Data Structure

The data which are connected to this report can be accessed via DOI:http://dx.doi.org/10.5880/GFZ.b103-15021.1.. All data of type 1 is stored

in a single .csv file format (data_type1.csv) where the time is stored in the first and the respective values in the following columns 7.1. Here, the date is given in DD.MM.YYYY and the time in hh:mm. The sensor for each column is given in the header row of the file. For data of type 2 and 3, Table 7.2 shows an example of the file structure. For types 2 and 3, a separate file was generated for each sensor. The file name gives the sensor. The time of each sample is stored in the first column of each file, the second column gives the respective measurement.

**Table 7.1.:** File structure for data of type 1 (data_type1.csv).

| |
|---|
| Date_Time;Strom_L1;... |
| 01.06.2011 00:00;0;... |
| 01.06.2011 00:01;0;... |
| 01.06.2011 00:02;0;... |
| ... |

**Table 7.2.:** File structure for data of type 2 and 3.

| |
|---|
| 01.06.2011 00:00;0 |
| 01.06.2011 00:01;0 |
| 01.06.2011 00:02;0 |
| ... |

# 8. Well Details

## 8.1. GrSk 4/05 (A2)

**Table 8.1.:** Well location of well GrSk 4/05 (A2) according to Brandt (2008) (converted to UTM-WGS94 Zone 33 using the software TRANSDAT).

| | |
|---|---|
| X-Coordinate | 405944.60 (m) |
| Y-Coordinate | 5862461.17 (m) |
| Ground level | 65.96 (m) |

**Table 8.2.:** Design of the production well GtGrSk 4/05 (A2) at the Groß Schönebeck research site.

| Bit Size (inch) | Depth (m, MD) |
|---|---|
| 23 | 744 |
| 16 | 2383 |
| 12 1/4 | 3160 |
| 8 1/2 | 3879 |
| 5 7/8 | 4400.4 |

| Casing | Size (inch) | Depth top ( m, MD) | Depth bottom ( m, MD) | Wall Thickn. (mm) | Weight (lbs/ft) | Grade | ID (mm) | Drift (mm) | Coupling |
|---|---|---|---|---|---|---|---|---|---|
| Cond. Casing | 660 mm | 0 | 41.6 | | | | | | |
| Surf. Casing | 18 5/8″ | 0 | 741.2 | 11.05 | 87.5 | L80/X56 | 450.98 | 446.2 | BTC |
| Prod. Casing | 16″ x | 0 | 723 | 14.61 | 96 | N80/HCN80 | 377.19 | 368.2 | Hydril521 |
| | 13 3/8″ x | 723 | 1680 | 13.06 | 72 | P110 | 313.61 | 311.15 | Hydril523 |
| | 13 5/8″ x | 1680 | 1803 | 15.88 | 88.2 | Q125 | 314.33 | 310.36 | NEW VAM |
| | 13 3/8″ | 1803 | 2381.5 | 13.06 | 72 | P110 | 313.61 | 311.15 | Hydril523 |
| Liner | 9 5/8″ | 2305.5 | 2570.9 | 13.85 | 53.5 | L80 | 216.79 | 215.9 | BTC |
| | | 2305.5 | 3886 | 13.85 | 53.5 | Q125 | 216.79 | 215.9 | BTC |
| Liner | 7″ x | 2333 | 2907 | 12.65 | 35 | L80 | 152.5 | 149.33 | BTC |
| | 7 5/8″ | 2907 | 3878 | 20.65 | 59.2 | P110 | 151.46 | 149.32 | VAMSLIJ2 |
| Liner | 5″ x | 3761 | 4355 | 9.19 | 18 | HC110 | 108.61 | | VAMFJL |
| | 5″(perf.) | 4355 | 4389 | 7.51 | 15 | C95 | 111.98 | | Hydrill511 |
| Prod. Tubing | 4 1/2″ x | 0 | 1159 | | 12.6 | J55 (coated) | | | VAGT |
| | 4 1/2″ | 1159 | 1163.3 | | 12.6 | 13Cr/J55 (Isol. joint) | | | VAM |



Scientific Technical Report STR 15/02 - Data
DOI: http://dx.doi.org/10.2312/GFZ.b103-15021

### 8.1.1. Dip and Azimuth

The dip and azimuth data from well Gt GrSk 4/05 (A2) can be accessed via DOI http://dx.doi.org/10.5880/GFZ.b103-15021.1.

# 8.2. E GrSk 3/90

**Table 8.3.:** Well location of well E GrSk 3/90 according to Brandt (2009) (converted to UTM-WGS94 Zone 33 using the software TRANSDAT).

| | |
|---|---|
| X-Coordinate | 405948.40 (m) |
| Y-Coordinate | 5862487.86 (m) |
| Ground level | 65.98 (m) |

**Table 8.4.:** Design of the injection well E GrSk 3/90 at the Groß Schönebeck research site.

| Bit Size (in) | Depth (m, MD) |
|---|---|
| 18 | 18 |
| 16 | 207.5 |
| 12 1/4 | 2375.5 |
| 8 1/2 | 3877 |
| 5 7/8 | 4309 |

| Casing | Size (inch) | Depth top (m, MD) | Depth bottom (m, MD) | Wall Thickness (mm) | Weight (lbs/ft) | Grade | ID (mm) | Drift (mm) | Coupling |
|---|---|---|---|---|---|---|---|---|---|
| Cond. Casing | 18 5/8″ | 0 | 18 | 11.05 | | | | | |
| Surf. Casing | 13 3/8v | 0 | 205 | 12.19 | | J55 | 315.32 | | K14 |
| Prod. Casing | 9 5/8″ | 0 | 2375 | 10-12 | | P110/D/E | | | LM/KM/ OTTM/LM |
| Liner | 7″ | 2309 | 3874 | 11.51 | | N80 | | | LM |
| Liner | 5″ x 5″ (perf.) | 3820 | 4305 | | 15 | L80 | | | BTC |
| Prod. Casing | 7″ | 0 | 2309 | 10.36 | 29 | L80 | 157.07 | 153.9 | BTC |
| Inj. Tubing | 4 1/2″ | 0 | 305 | | 12.6 | J55 | | | VAGT |

## 8.2.1. Dip and Azimuth

The dip and azimuth data from well E GrSk 3/90 can be accessed via DOI http://dx.doi.org/10.5880/GFZ.b103-15021.1.

# 9. Gas flow rate

The following pages show the calibration sheet for the rented rotary displacement meter (Drehkolbenzähler) RM-A G250 as well as pictures of the additionally installed pressure and temperature sensors during the calibration measurements.



Scientific Technical Report STR 15/02 - Data
DOI: http://dx.doi.org/10.2312/GFZ.b103-15021

## Prüfergebnisprotokoll

**Gas Service Freiberg GmbH**
**Halsbrücker Str. 34**
**09599 Freiberg**
**Tel.: 03731 365 330**

| | | | | |
|---|---|---|---|---|
| **Prüfung:** | Art: **Eichung** | | Prüfer: **Preußer** | Prüfanlage: **TRZ-Prüfstand** |
| | Datum: **22.07.13** | | Prüfnummer: **13** | |
| **Prüfling:** | Gerätetyp: **Drehkolbenzähler** | | 1 tr = | |
| | Größe: **RM-A G250** | | Zählwerkssatz: | |
| | Nennweite: **DN 100** | | Justierradsatz J1/J2: | |
| | Druckstufe: **PN 16** | | Bauart: **7.131/92.04** | |
| | Fabrik-Nr.: **300676** | | WME: **-0.01 %** | |
| | Baujahr: **1993** | | Flußrichtung: **links-rechts Doppelzählwe** | |

| Impulsgeber: | Anzahl | Gebertyp | Impulswert | Max. Frequenz |
|---|---|---|---|---|
| | | A1S | imp/m³ | Hz |
| | | A1R | imp/m³ | Hz |
| | | E300 | imp/m³ | Hz |
| | **1** | INS/E1 | **1.00** imp/m³ | **0.11** Hz |
| | **1** | INS/E1 | **1.00** imp/m³ | **0.11** Hz |
| | | E200 | imp/m³ | Hz |

**Meßergebnisse:**

| | | Temp | Druck | Volumen-durchfluß | Meßab-weichung |
|---|---|---|---|---|---|
| | | °C | mbar | m³/h | % |
| Prüfp. | 1 | **20.37** | **3.59** | **404.57** | **-0.01** |
| Prüfp. | 2 | **20.54** | **1.99** | **283.47** | **0.00** |
| Prüfp. | 3 | **20.62** | **1.05** | **167.44** | **-0.06** |
| Prüfp. | 4 | **20.67** | **0.63** | **98.75** | **-0.05** |
| Prüfp. | 5 | **20.38** | **0.49** | **42.00** | **0.14** |
| Prüfp. | 6 | **20.57** | **0.42** | **20.13** | **0.24** |
| Prüfp. | 7 | **20.66** | **0.41** | **2.48** | **-0.08** |
| Prüfp. | ZWK | **20.67** | **3.64** | **402.31** | **0.03** |

**Normale:**

| Bez.: | Fabrik-Nr.: | Größe: | Impulswert: | Meßbereich: |
|---|---|---|---|---|
| **N1** | **83028964** | **G1000** | **5314.440 imp/m³** | **90 - 1600 m³/h** |
| **N2** | **62930131** | **G65** | **9808.500 imp/m³** | **7 - 120 m³/h** |
| **N3** | **300234** | **NB15** | **10000.000 imp/m³** | **0.2 - 17.5 m³/h** |

Ausdruck erstellt am: 22.07.13

Unterschrift

**Gas Service Freiberg GmbH**
**Halsbrücker Straße 34**
**09599 Freiberg**
**Telefon 03731 365330**

Gas Service Freiberg GmbH Halsbrücker Str. 34 09599 Freiberg Tel. 03731 365 330

**Gas Service**

**Freiberg GmbH**

| | |
|---|---|
| **Kunde:** | Deutsches GeoForschungsZentrum GFZ |
| **Auftrags - Nr.:** | DKZ 001/DGF |

# Abnahmeprüfzeugnis

**Bescheinigung nach EN 10204 - 3.1**

Acceptance Test certificate According to EN 10204 - 3.1 / Certificat de Réception selon EN 10204 - 3.1

| | | | | |
|---|---|---|---|---|
| **Drehkolbenzähler** | IRM-A G250 | | **Fabrik - Nr.** | 300676 |
| **Nennweite** | DN 100 | | **Baujahr** | 1993 |
| **Druckstufe** | **PN** | 16 | **Ausführung** | |
| **höchstzulässiger Betriebsdruck** | **bar** | 16 | **zulässiger Betriebstemperatur - Bereich - 20 bis + 60° C** | |
| **zulässige Gasart** | **Erdgas** | | | |

**Nur Gase gemäß DVGW - Arbeitsblatt G 260/I; Sauerstoff, Atzetylen, aggressive oder toxische Gase sind nicht zulässig**

## Funktionsprüfung

| | | | | |
|---|---|---|---|---|
| **Meßbereich** | **Qmin** | 2.5 m³/h | **Qmax** | 400 m³/h |
| **Bauartzulassung** | 7.131/92.04 | | | |

## Dichtheitsprüfung

**Anforderungen : DIN EN 12261**

| | | |
|---|---|---|
| **Dichtheitsprüfung** | 18 | **bar** |

Das Gerät ist gemäß der Daten auf Dichtheit geprüft und für einwandfrei befunden

## Impulsgeber

| | | | | | |
|---|---|---|---|---|---|
| **1. E1** | **1 m³** | **=** | **1.00 Imp** | **fmax =** | **0.11 HZ** |
| **2. E1** | **1 m³** | **=** | **1.00 Imp** | **fmax =** | **0.11 HZ** |
| **E 300** | **1 m³** | **=** | **Imp** | **fmax =** | **HZ** |
| **E 200** | **1 m³** | **=** | **Imp** | **fmax =** | **HZ** |
| **A1R** | **1 m³** | **=** | **Imp** | **fmax =** | **HZ** |
| **A1S** | **1 m³** | **=** | **Imp** | **fmax =** | **HZ** |
| **$t_R$** | **1 m³** | **=** | **Imp** | **fmax =** | **HZ** |
| **ZW Absolut Encoder** | **1 m³** | **=** | **Imp** | **fmax =** | **HZ** |

**Abnahmebeauftragter**

**Gas Service Freiberg GmbH**
**Halsbrücker Straße 34**
**09599 Freiberg**
**Telefon 03731 365330**

**Datum / Date :** 22.07.13



Gas Service Freiberg
Halsbrücker Str. 34 09599 Freiberg
Tel. 03731 365 330 Fax 03731 365 407

Deutsches GeoForschungsZentrum GFZ

**Staatlich anerkannte Prüfstelle für Messgeräte für Gas GR 5**
**bei der GSF - Gas Service Freiberg GmbH**

**DIE BEI DEN MESSUNGEN VERWENDETEN NORMALE SIND AUF DIE NATIONALEN NORMALE BEI DER PHYSIKALISCH-TECHNISCHEN BUNDESANSTALT RÜCKGEFÜHRT.**
*THE STANDARDS USED FOR THE MEASUREMENTS ARE TRACEABLE TO THE NATIONAL STANDARDS AT THE PHYSIKALISCH-TECHNISCHE BUNDESANSTALT.*

# Eichschein

*Verification certificate*

**Nummer** *Number* **255/13**

**Gegenstand** *Object* **Drehkolbenzähler**

**Identifikation** *Identification* **IRM-A G250** **300676**

**Hersteller** *Manufacturer* **Instromet**

**Antragsteller** *Applicant* **Deutsches GeoForschungsZentrum GFZ**

**Prüfverfahren** *Test procedure*
Der Drehkolbenzähler wurde nach den PTB-Prüfregeln Band29 Abschnitt 6.1 - 6.3 geprüft. Dabei wurde er in Reihenschaltung mit Volumengaszähler-Gebrauchsnormalen unter Benutzung der Impulsgeber am Normal und Prüfling verglichen. Maßgeblich für den Zustand der Prüfluft waren dabei die Drücke am"pr-Stutzen" und die Temperaturen am Ausgang der Zähler.

**Ergebnis** *Result* **Die Anforderungen der Eichordnung Anlage 7-1 wurden erfüllt.**

**Ort und Datum der Eichung** *Place and date of verification* **Freiberg, den 22.07.2013**

GR 5 13

**Gültigkeit der Eichung bis** *This verification is valid until* **31.12.2029**

**Stempelzeichen** *Marking*

Die Gültigkeit der Eichung erlischt vorzeitig, wenn eine der in §13 Absatz 1 der Eichordnung beschriebenen Veränderungen eingetreten ist.
*The validity of the verification has ceased to exist if one of the changes listed in §13 section 1 of the Eichordnung has occured.*

**Eichscheine ohne Unterschrift und Dienstsiegel haben keine Gültigkeit.**
**Dieser Eichschein darf nur unverändert weiterverbreitet werden.**
*Verification certificates without signature and official stamp are not valid. This verification certificate may only be reproduced in unchanged form.*

Ort und Datum
*Place and date*
Freiberg,den 24.07.2013

Dienstsiegel
*Official stamp*
STAATLICH ANERKANNTE PRÜFSTELLE GR 5 FREIBERG

(Name)
*On behalf of*
i.V. i.A.

Staatlich anerkannte Prüfstelle für Messgeräte für Gas GR 5 bei der GSF - Gas Service Freiberg GmbH
Sitz: Halsbrücker Str. 34 ; 09599 Freiberg
Tel.: 03731 365 330 ; Fax: 03731 365 407 ; e-Mail: info@gsf-freiberg.de

Scientific Technical Report STR 15/02 - Data
DOI: http://dx.doi.org/10.2312/GFZ.b103-15021

# Bedienungsanleitung unbedingt beachten!

- Es dürfen **keine Schwebteile** im Gas enthalten sein – außerdem muss das **Gas trocken** sein. Andernfalls kann der Zähler Schaden nehmen.

-Zum Schutz des Zählers muss in Neuanlagen ein Grobfilter (Siebdichtung) eingebaut sein, für bereits bestehende Anlagen ist dies zu empfehen. Das Sieb **sollte nach ca. 4 bis 6 Wochen entfernt werden.**

Montieren Sie den Zähler:

- gasdicht,
- mit den mitgelieferten Zubehörteilen,
- nur in **Durchflussrichtung** (entsprechend der Kennzeichnung durch einen Pfeil am Zählergehäuse oder Zählwerkskopf),
- nur **verspannungsfrei**,
- die Achsen der Kolben müssen sich in **horizontaler Position** befinden
- achten Sie beim Einsetzen der Dichtungen darauf, dass diese **konzentrisch ausgerichtet** sind und nicht in den Strömungskanal hinein ragen,
- wettergeschützt

- **Vor der Inbetriebnahme Öl einfüllen.**
- Zum Einfüllen des Öles machen Sie den Zähler **drucklos.**
- Füllen Sie das Öl mit der Spritze langsam ein. Es dauert 5 bis 10 Minuten, bis das Öl in beiden Ölkammern das gleicheNiveau erreicht. Die Ölmenge ist korrekt, wenn sich der Ölstand im unteren Drittel des Schauglases befindet.
- Im laufenden Betrieb wird das Öl im Zähler verteilt, u.U. ist kein Öl im Schauglas zu erkennen. Aus diesem Grund muss die Kontrolle des Ölstandes im Stillstand des Zählers nach ca. 5 Minuten erfolgen. Zum Nachfüllen muss der Zähler drucklos sein.
- **Transportieren Sie einen Drehkolbengaszähler nie mit Öl.** Lassen Sie das Öl unbedingt ab, **sonst** gelangt das Öl in den Messraum und **beschädigt** den Zähler.

- **Befüllen** Sie die Anlage **langsam** bis zum Erreichen des Betriebsdrucks.
- Der **Druckanstieg** darf 350 mbar/s nicht übersteigen.
- Überschreiten Sie den **Messbereich** auch nicht kurzzeitig!

Es dürfen **keine Schwebteile** im Gas enthalten sein – außerdem muss das **Gas trocken** sein. Andernfalls kann der Zähler Schaden nehmen.

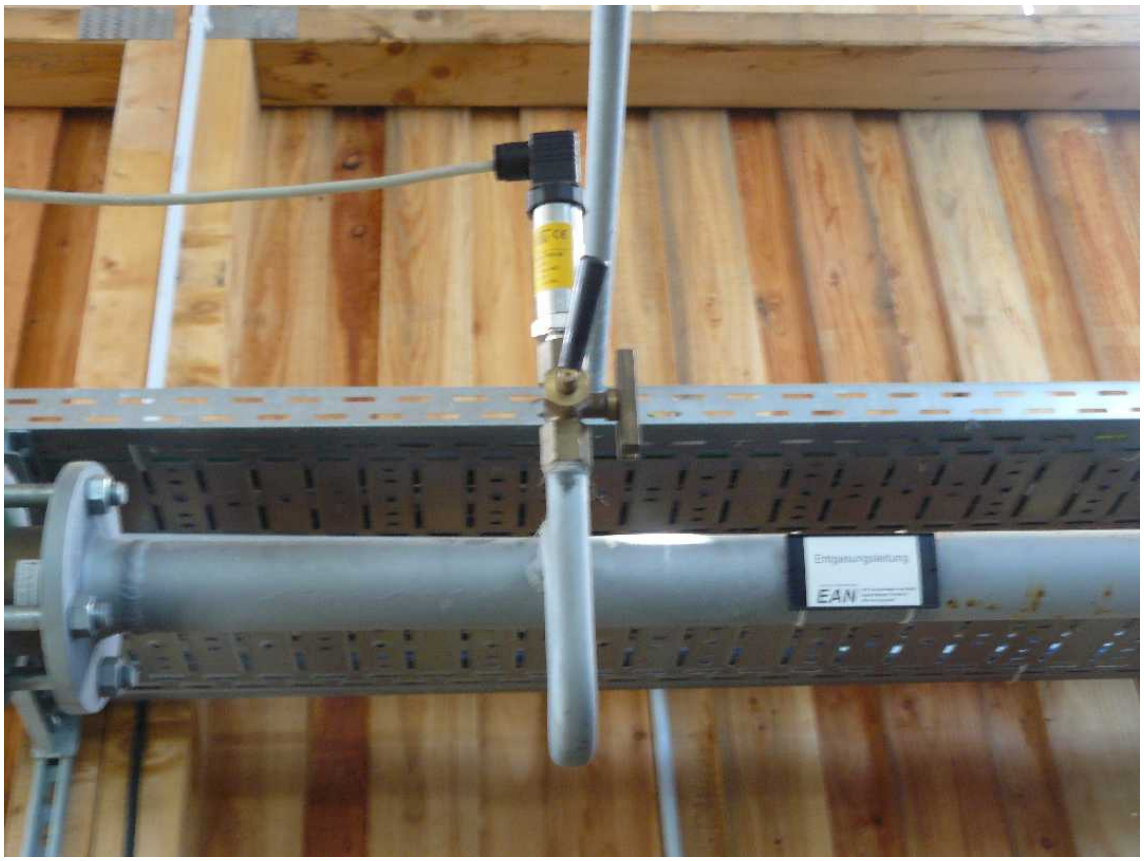


**Figure 9.1.:** Additional pressure sensor to monitor the pressure after the degasser.



Scientific Technical Report STR 15/02 - Data
DOI: http://dx.doi.org/10.2312/GFZ.b103-15021

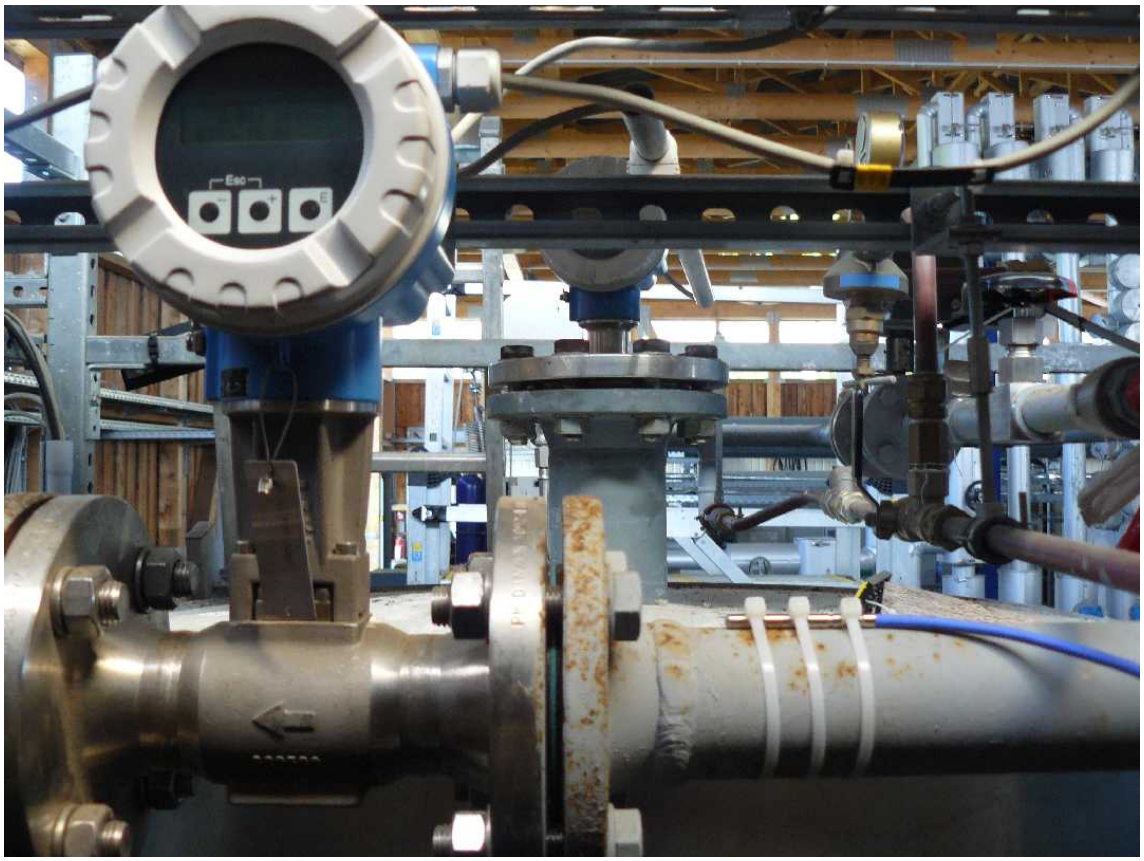

**Figure 9.2.:** Temperature sensor on flow line attached to pipe with ties.



Scientific Technical Report STR 15/02 - Data
DOI: http://dx.doi.org/10.2312/GFZ.b103-15021

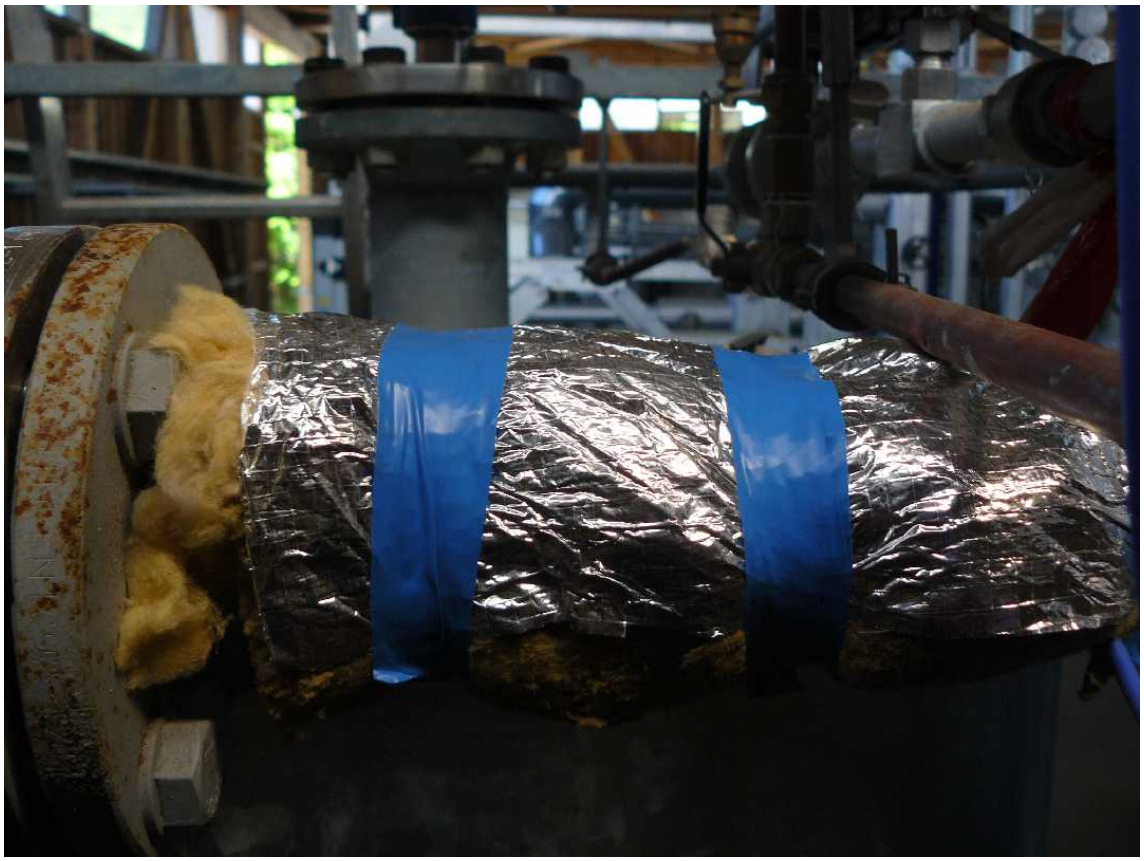

**Figure 9.3.:** Temperature sensor under insulation on flow line.



Scientific Technical Report STR 15/02 - Data
DOI: http://dx.doi.org/10.2312/GFZ.b103-15021

# 10. Related Publications


- Banks, J. (2013). Sulfate mineral scaling during the production of geothermal energy from sedimentary basin formation brines : a case study at the Groß Schönebeck in-situ geothermal laboratory, Germany. PhD Thesis, FU Berlin

- Bauer, K., Moeck, I., Norden, B., Schulze, A., Weber, M., & Wirth, H. (2010). Tomographic P wave velocity and vertical velocity gradient structure across the geothermal site Groß Schönebeck (NE German Basin): Relationship to lithology, salt tectonics, and thermal regime. Journal of Geophysical Research: Solid Earth, 115(8). http://dx.doi.org/10.1029/2009jb006895

- Bauer, K., Muñoz, G., & Moeck, I. (2012). Pattern recognition and lithological interpretation of collocated seismic and magnetotelluric models using self-organizing maps. Geophysical Journal International, 189(2), 984-998. http://dx.doi.org/10.1111/j.1365-246X.2012.05402.x

- Blöcher, G., Zimmermann, G., & Milsch, H. (2009). Impact of poroelastic response of sandstones on geothermal power production. Pure and Applied Geophysics, 166(5-7), 1107-1123. http://dx.doi.org/10.1007/s00024-009-0475-4

- Blöcher, M. G., Zimmermann, G., Moeck, I., Brandt, W., Hassanzadegan, A., & Magri, F. (2010). 3D numerical modeling of hydrothermal processes during the lifetime of a deep geothermal reservoir. Geofluids, 10(3), 406-421. http://dx.doi.org/10.1111/j.1468-8123.2010.00284.x

- Bruhn, D. (2008). The European I-GET project on integrated geophysical exploration methods for geothermal systems. Paper presented at the Transactions - Geothermal Resources Council.

- Cherubini, Y., Cacace, M., Scheck-Wenderoth, M., Moeck, I., & Lewerenz, B. (2013). Controls on the deep thermal field; implications from 3-D numerical simulations for the geothermal research site Gross Schonebeck. Environmental Earth Sciences, 70(8), 3619-3642. http://dx.doi.org/10.1007/s12665-013-2519-4

- Deon, F., Regenspurg, S., & Zimmermann, G. (2013). Geochemical interactions of Al2O3-based proppants with highly saline geothermal brines at simu-

lated in situ temperature conditions. Geothermics, 47, 53-60. http://dx.doi.org/10.1016/j.geothermics.2013.02.003

- Evans, K. F., Zappone, A., Kraft, T., Deichmann, N., & Moia, F. (2012). A survey of the induced seismic responses to fluid injection in geothermal and CO2 reservoirs in Europe. Geothermics, 41, 30-54. http://dx.doi.org/10.1016/j.geothermics.2011.08.002

- Feldbusch, E., Regenspurg, S., Banks, J., Milsch, H., & Saadat, A. (2013). Alteration of fluid properties during the initial operation of a geothermal plant: Results from in situ measurements in Groß Schönebeck. Environmental Earth Sciences, 70(8), 3447-3458. http://dx.doi.org/10.1007/s12665-013-2409-9

- Francke, H., Kraume, M., & Saadat, A. (2013). Thermal-hydraulic measurements and modelling of the brine circuit in a geothermal well. Environmental Earth Sciences, 70(8), 3481-3495. http://dx.doi.org/10.1007/s12665-013-2612-8

- Frick, S., Regenspurg, S., Kranz, S., Milsch, H., Saadat, A., Francke, H., Brandt, W., & Huenges, E. (2011). Geochemical and process engineering challenges for geothermal power generation. Chemie-Ingenieur-Technik, 83(12), 2093-2104. http://dx.doi.org/10.1002/cite.201100131

- Gehrke, D. (2006). Thermisch-hydraulische 3D Modellierung des geothermischen Reservoirs um die Dublette (E GrSk 03/90 / Gt GrSk 04/05) von Groß Schönebeck unter Berücksichtigung von Stimulationsmaßnahmen (S.). Greifswald.

- Henninges, J., Brandt, W., Erbas, K., Moeck, I., Saadat, A., Reinsch, T., Zimmermann, G., & ICGR International Center for Geothermal Research, G. C., GFZ Publication Database, Deutsches GeoForschungsZentrum,. (2012). Downhole monitoring during hydraulic experiments at the in-situ geothermal lab Gross Schönebeck. Paper presented at the 37th Workshop on Geothermal Reservoir Engineering (Stanford, USA 2012), Stanford.

- Huenges, E., Erbas, K., Moeck, I., Blöcher, G., Brandt, W., Schulte, T., Saadat, A., Kwiatek, G., & Zimmermann, G. (2009). The EGS project Groß Schönebeck - Current status of the large scale research project in Germany. Paper presented at the 33rd Annual Meeting Geothermal Resources Council (Reno, USA 2009).

- Huenges, E., Holl, H.-G., Legarth, B., Zimmermann, G., Saadat, A., & Tischner, T. (2004). Hydraulic stimulation of a sedimentary geothermal reservoir in the North German Basin; case study Gross Schoenebeck. Zeitschrift fuer Angewandte Geologie, 50(2), 24-27.

- Huenges, E., Holl, H.-G., Legarth, B. A., Zimmermann, G., & Saadat, A. (2004). The stimulation of a sedimentary geothermal reservoir in the North German Basin: case study Groß Schönebeck. Paper presented at the Twenty-Ninth Workshop on Geothermal Reservoir Engineering (Stanford, USA 2004), Stanford.

- Huenges, E., & Hurter, S. (2002). In-situ Geothermielabor Groß Schönebeck 2000/2001 : Bohrarbeiten, Bohrlochmessungen, Hydraulik, Formationsfluide, Tonminerale (Bd. 02/14). Potsdam: GeoForschungsZentrum.

- Huenges, E., Moeck, I., Saadat, A., Brandt, W., Schultz, A., Holl, H.-G., Bruhn, D., Zimmermann, G., Bloecher, G., & Wohlgemuth, L. (2007). Directional drilling and stimulation of a deep sedimentary geothermal reservoir. Scientific Drilling, 5, 47-49. http://dx.doi.org/10.2204/iodp.sd.5.08.2007

- Huenges, E., Moeck, I., Saadat, A., Brandt, W., Schulz, A., Bruhn, D., Holl, H. G., Zimmermann, G., Blöcher, G., & Wohlgemuth, L. (2007). Geothermal research well in a deep sedimentary reservoir. Paper presented at the Transactions - Geothermal Resources Council.

- Huenges, E., Saadat, A., Brandt, W., Moeck, I., Holl, H.-G., Zimmermann, G., Blöcher, G., Köhler, S., Legarth, B., & Tischner, T. (2006). Current status of the EGS Gross Schönebeck project: on the way to demonstrate sustainable brine production from deep sediments of the North German basin. Paper presented at the Geothermal Resources Council 2006 Annual Meeting (San Diego, USA 2006).

- Huenges, E., Saadat, A., Köhler, S., Trautwein, U., & Hurter, S. (2002). The in-situ geothermal laboratory Groß Schönebeck: learning to use low permeability aquifers for geothermal power. Paper presented at the 27th Workshop Geothermal Reservoir Engineering (Stanford 2002), Stanford (CA), USA.

- Huenges, E., Trautwein, U., Legarth, B., & Zimermann, G. (2006). Fluid pressure variation in a sedimentary geothermal reservoir in the North German Basin; case study Gross Schoenebeck. Pure and Applied Geophysics, 163(10), 2141-2152. http://dx.doi.org/10.1007/s00024-006-0122-2

- Huenges, E., & Winter, H. (2004). Experimente zur Produktivitätssteigerung in der Geothermie-Forschungsbohrung Groß Schönebeck 3/90 (Bd. 04/16). Potsdam: GeoForschungsZentrum.

- Huenges, E., & Wolfgramm, M. (2004). Sandsteine im In-situ-Geothermielabor Groß Schönebeck : Reservoircharakterisierung, Stimulation, Hydraulik und Nutzungskonzepte (Bd. 04/03). Potsdam: GeoForschungsZentrum.

- Huenges, E., Zimmermann, G., Reinicke, A., Blöcher, G., Holl, H. G., Legarth, B., Saadat, A., Möck, I., Winter, H., Brandt, W., Köhler, S., Spalek, A., Poser, M., Schrötter, J., & Becker, R. (2006). Technologieentwicklung im In-Situ-Geothermielabor Groß Schönebeck Zweijahresbericht 2004/2005 (S. 103 - 112): GeoForschungszentrum Potsdam.

- Hurter, S., Koehler, S., Saadat, A., Holl, H.-G., Rockel, W., Trautwein, U., Zimmermann, G., Wolfgramm, M., Huenges, E., & Bloomquist, R. G. (2002). Stimulating low permeability aquifers; experiments in Rotliegend sandstones (NE Germany). Transactions - Geothermal Resources Council, 26, 215-220.

- Hurter, S., Köhler, S., Saadat, A., Trautwein, U., & Huenges, E. (2002). Das in-situ-Geothermielabor in der Bohrung Groß Schönebeck Zweijahresbericht GeoForschungsZentrum Potsdam 2000/2001 (S.).

- Kwiatek, G., Bohnhoff, M., Dresen, G., Schulze, A., Schulte, T., Zimmermann, G., & Huenges, E. (2010). Microseismicity induced during fluid-injection; a case study from the geothermal site at Gross Schoenebeck, North German Basin. Acta Geophysica, 58(6), 995-1020. http://dx.doi.org/10.2478/s11600-010-0032-7

- Legarth, B., Huenges, E., & Zimmermann, G. (2005). Hydraulic fracturing in a sedimentary geothermal reservoir; results and implications. International Journal of Rock Mechanics and Mining Sciences, 42(7-8), 1028-1041. http://dx.doi.org/10.1016/j.ijrmms.2005.05.014

- Legarth, B., Tischner, & T., Huenges, E. (2003): Stimulation experiments in sedimentary, low-enthalpy reservoirs for geothermal power generation, Germany. Geothermics, 32(4-6), 487-495. http://dx.doi.org/10.1016/j.geothermics.2003.07.007

- Milsch, H., Giese, R., Poser, M., Kranz, S., Feldbusch, E., & Regenspurg, S. (2013). Technical paper: FluMo-a mobile fluid-chemical monitoring unit for geothermal plants. Environmental Earth Sciences, 70(8), 3459-3463. http://dx.doi.org/10.1007/s12665-013-2408-x

- Milsch, H., Seibt, A., & Spangenberg, E. (2009). Long-term petrophysical investigations on geothermal reservoir rocks at simulated In situ conditions. Transport in Porous Media, 77(1), 59-78. http://dx.doi.org/10.1007/s11242-008-9261-5

- Moeck, I., Kwiatek, G., & Zimmermann, G. (2009): Slip tendency analysis, fault reactivation potential and induced seismicity in a deep geothermal reservoir. Journal of Structural Geology, 31(10), 1174-1182. http://dx.doi.org/10.1016/j.jsg.2009.06.012

- Moeck, I., & Backers, T. (2011). Fault reactivation potential as a critical factor during reservoir stimulation. First Break, 29(5), 73-80. http://dx.doi.org/10.3997/1365-2397.2011014

- Moeck, I., Schandelmeier, H., & Holl, H. G. (2009). The stress regime in a Rotliegend reservoir of the Northeast German Basin. International Journal of Earth Sciences, 98(7), 1643-1654. http://dx.doi.org/10.1007/s00531-008-0316-1

- Muñoz, G., Bauer, K., Moeck, I., Schulze, A., & Ritter, O. (2010). Exploring the Groß Schönebeck (Germany) geothermal site using a statistical joint interpretation of magnetotelluric and seismic tomography models. Geothermics, 39(1), 35-45. http://dx.doi.org/10.1016/j.geothermics.2009.12.004

- Munoz, G., & Ritter, O. (2013). Pseudo-remote reference processing of magnetotelluric data; a fast and efficient data acquisition scheme for local arrays. Geophysical Prospecting, 61(SUPPL. 1), 300-316. http://dx.doi.org/10.1111/1365-2478.12012

- Muñoz, G., Ritter, O., & Moeck, I. (2010). A target-oriented magnetotelluric inversion approach for characterizing the low enthalpy Groß Schönebeck geothermal reservoir. Geophysical Journal International, 183(3), 1199-1215. http://dx.doi.org/10.1111/j.1365-246X.2010.04795.x

- Noack, V., Cherubini, Y., Scheck-Wenderoth, M., Lewerenz, B., Höding, T., Simon, A., & Moeck, I. (2010). Assessment of the present-day thermal field (NE German Basin)-Inferences from 3D modelling. Chemie der Erde - Geochemistry, 70(SUPPL. 3), 47-62. http://dx.doi.org/10.1016/j.chemer.2010.05.008

- Ollinger, D., Baujard, C., Kohl, T., & Moeck, I. (2010). Distribution of thermal conductivities in the Groß Schönebeck (Germany) test site based on 3D inversion of deep borehole data. Geothermics, 39(1), 46-58. http://dx.doi.org/10.1016/j.geothermics.2009.11.004

- Regenspurg, S., Banks, J., & Zimmermann, G. (2010). Mineral precipitation from geothermal brines during reservoir activities - Example Gross Schonebeck (Germany). Geochimica et Cosmochimica Acta, 74(12), A856-A856.

- Regenspurg, S., Dilling, J., Mielcarek, J., Korte, F., & Schkade, U. K. (2014). Naturally occurring radionuclides and their geochemical interactions at a geothermal site in the North German Basin. Environmental Earth Sciences, 72(10), 4131-4140. http://dx.doi.org/10.1007/s12665-014-3306-6

- Regenspurg, S., Feldbusch, E., Byrne, J., Deon, F., Driba, D. L., Henninges, J., Kappler, A., Naumann, R., Reinsch, T., & Schubert, C. (2015). Mineral precipitation during production of geothermal fluid from a Permian Rotliegend reservoir. Geothermics, 54, 122-135. http://dx.doi.org/10.1016/j.geothermics.2015.01.003

- Regenspurg, S., Milsch, H., Giese, R., & Poser, M. (2011). Monitoring fluid properties in a geothermal plant. Mineralogical Magazine, 75(3), 1703.

- Regenspurg, S., Milsch, H., Schmidt, K., Saadat, A. & Huenges, E. (2009). Corrosion and scaling in low-enthalpy geothermal systems in northern Germany. Geochimica et Cosmochimica Acta, 73(13S), A1081.

- Regenspurg, S., Wiersberg, T., Brandt, W., Huenges, E., Saadat, A., Schmidt, K., & Zimmermann, G. (2010). Geochemical properties of saline geothermal fluids from the in-situ geothermal laboratory Groß Schönebeck (Germany). Chemie der Erde - Geochemistry, 70(SUPPL. 3), 3-12. http://dx.doi.org/10.1016/j.chemer.2010.05.002

- Reinicke, A., Zimmermann, G., Huenges, E., & Burkhardt, H. (2005). Estimation of hydraulic parameters after stimulation experiments in the geothermal reservoir Groß Schönebeck 3/90 (North-German Basin). International Journal of Rock Mechanics and Mining Sciences, 42(7-8 SPEC. ISS.), 1082-1087. http://dx.doi.org/10.1016/j.ijrmms.2005.05.009

- Reinsch, T., Regenspurg, S., Feldbusch, E., Saadat, A., Huenges, E., Erbas, K., Zimmermann, G., & Henninges, J. (2015) Reverse Cleanout in a Geothermal Well: Analysis of a Failed Coiled-Tubing Operation. SPE Production & Operations, http://dx.doi.org/10.2118/174080-PA

- Reinsch, T., Kranz, S., Saadat, A., Huenges, E, Rinke, M., Brandt, W., & Schulz, P. (2015) Balanced reverse cleanout operation - removing large and heavy particles from a geothermal well. SPE Production & Operations, (submitted)

- Urpi, L., Zimmermann, G., Blöcher, G., & Kwiatek, G. (2011). Microseismicity at Groß Schönebeck - a Case Review. Paper presented at the 36th Workshop on Geothermal Reservoir Engineering (Stanford, USA 2011).

- Yoon, J. S., Zimmermann, G., & Zang, A. (2015). Numerical Investigation on Stress Shadowing in Fluid Injection-Induced Fracture Propagation in Naturally Fractured Geothermal Reservoirs. Rock Mechanics and Rock Engineering. http://dx.doi.org/10.1007/s00603-014-0695-5

- Zimmermann, G., Blöcher, G., Reinicke, A., & Brandt, W. (2011). Rock specific hydraulic fracturing and matrix acidizing to enhance a geothermal system - Concepts and field results. Tectonophysics, 503(1-2), 146-154. http://dx.doi.org/10.1016/j.tecto.2010.09.026

- Zimmermann, G., Hurter, S., Saadat, A., Köhler, S., Trautwein, U., Holl, H.-G., Wolfgramm, M., Winter, H., Legarth, B. A., & Huenges, E. (2003). The in-situ geothermal laboratory Groß Schönebeck - Stimulation of sandstones in 4200 m depth. Paper presented at the 28th Workshop on Geothermal Reservoir Engineering (Stanford 2003), Stanford, CA, USA.

- Zimmermann, G., & Moeck, I. (2008). Geothermie Forschungsbohrung in Gross Schoenebeck; von der Planung bis zur Stimulation. Brandenburgische Geowissenschaftliche Beitraege, 15(1-2), 155-164.

- Zimmermann, G., Moeck, I., & Blöcher, G. (2010). Cyclic waterfrac stimulation to develop an Enhanced Geothermal System (EGS)-Conceptual design and experimental results. Geothermics, 39(1), 59-69. http://dx.doi.org/10.1016/j.geothermics.2009.10.003

- Zimmermann, G., & Reinicke, A. (2010). Hydraulic stimulation of a deep sandstone reservoir to develop an enhanced geothermal system; laboratory and field experiments. Geothermics, 39(1), 70-77. http://dx.doi.org/10.1016/j.geothermics.2009.12.003

- Zimmermann, G., Reinicke, A., Blöcher, G., Milsch, H., Gehrke, D., Holl, H.-G., Moeck, I., Brandt, W., Saadat, A., & Huenges, E. (2007). Well path design and stimulation treatments at the geothermal research well GtGrSk4/05 in Groß Schönebeck. Paper presented at the 32nd Workshop on Geothermal Reservoir Engineering (Stanford, USA 2007), Stanford.

- Zimmermann, G., Tischner, T., Legarth, B., & Huenges, E. (2009). Pressure-dependent production efficiency of an Enhanced Geothermal System (EGS): Stimulation results and implications for hydraulic fracture treatments. Pure and Applied Geophysics, 166(5-7), 1089-1106. http://dx.doi.org/10.1007/s00024-009-0482-5

ISSN 2190-7110